Throwing shade: Physiological responses to light explain competition and facilitation in a tree diversity experiment

Shan Kothari,[1*] Rebecca Montgomery,[2] Jeannine Cavender-Bares[1,3]

[1]Department of Plant and Microbial Biology, University of Minnesota, 140 Gortner Laboratory, 1479 Gortner Ave., St. Paul, MN, 55108
[2]Department of Forest Resources, University of Minnesota, St. Paul, MN, 55108
[3]Department of Ecology, Evolution, and Behavior, University of Minnesota, St. Paul, MN, 55108

*corresponding author
Email: kotha020@umn.edu
Phone: (734) 502-2817

Author contributions: SK conceived the project with JCB, conducted physiological measurements, analyzed and interpreted the data with JCB and RM, and wrote the first draft of the paper. JCB and RM designed the FAB experiment, coordinated annual biomass surveys, and contributed to subsequent revisions of the paper.

Summary

- Interspecific facilitation is often invoked in explanations of biodiversity-ecosystem function relationships in plant communities, but it is seldom clear how it occurs. Physiological experiments show that excess light causes stress that may depress long-term carbon assimilation. If shading by a plant's neighbors reduces light stress, it may facilitate that plant's growth. On the other hand, when light is a limiting factor for growth, shading will often have a net negative, competitive effect.
- In a tree diversity experiment, we measured growth rates and photosynthetic physiology of broadleaf tree species across a gradient of light availability imposed by their neighbors. At the extremes, trees experienced nearly full sun (monoculture), or were shaded by nearby fast-growing conifers (shaded biculture).
- Although most species had lower growth with larger neighbors, implying a net competitive effect, the two most shade-tolerant species (*Tilia americana* and *Acer negundo*) had positive responses to neighbor size. Compared to the others, these two species were especially susceptible to photoinhibition (reduced dark-acclimated F_v/F_m) in full sun. While most species had lower

assimilation rates in shaded bicultures, *T. americana* had carbon assimilation rates up to 25% higher. *T. americana* also dropped its leaves 3-4 weeks later in the shaded biculture, extending its growing season. We conclude that although large neighbors can cause light limitation in shade-intolerant species, they can also increase growth through abiotic stress amelioration in shade-tolerant species.

- Both positive and negative species interactions in our experiment can be explained by the photosynthetic responses of trees to the light environment created by their neighbors. We show that physiological measurements can deepen our understanding of the species interactions that underlie biodiversity-ecosystem function relationships.

Keywords: Photoprotection; photoinhibition; photosynthetic light-response curves; competition; facilitation; tree diversity; biodiversity and ecosystem function

Introduction

The sun's light powers photosynthesis, the chain of reactions through which plants turn carbon dioxide into the living matter they use to grow and reproduce. A dominant view in plant ecology is that light is often a limiting resource, and competition for scarce light shapes the fate of plant species (Braun-Blanquet 1932; Canham et al. 1994; Monsi & Saeki 2005; Dybzinski & Tilman 2007). While this is often true, physiologists have also shown that, as other factors begin to limit photosynthesis, plants often absorb more light than they are able to use. Beyond an initial linear rise with increasing light availability, photosynthesis begins to saturate, such that additional light contributes little to the plant's carbon gain. Moreover, external factors that limit photosynthesis—including water limitation, cold temperatures, or nutrient-poor conditions—can exacerbate this excess of light (Fig. 1; Long et al. 1991; Demmig-Adams & Adams 1992; Demmig-Adams & Adams 2018).

Light is thus both an essential resource and a potential stressor. A chronic excess of light can cause lasting oxidative damage to plant cells, especially Photosystem II (PSII), and this damage reduces the efficiency of photosynthesis. Plants can avoid damage through mechanisms of photoprotection. These include biochemical pathways that shunt off excess light safely as heat—most notably, the xanthophyll cycle. They also include structural means of avoiding excess light interception, such as self-shading, reflective leaves, or steep leaf angles (Lovelock et al. 1992; Pearcy et al. 2005; Kothari et al. 2018). However, once induced, many forms of biochemical photoprotection are slow to reverse. Even when light conditions are no longer stressful, these mechanisms may continue to suppress photosynthesis for some time (Demmig-Adams and Adams 2006; Kromdijk et al. 2016). Similarly, structural mechanisms like self-shading may be costly under low ambient light. In general, photoprotective ability often increases with exposure to conditions that put plants at risk of damage in the habitat of origin, including high light (Montgomery et al. 2008) and cold or dry conditions (Cavender-Bares 2007; Savage et al. 2009; Wujeska et al. 2013; Ramírez-Valiente et al. 2013). In these environments, photoprotection may be necessary to prevent even more costly damage.

Depending on a plant's level of investment in photoprotection, these mechanisms may lack the capacity to protect against prolonged exposure to excess light, which can reduce net carbon assimilation rates (Egerton et al. 2000; Howell et al. 2002; Murchie & Niyogi 2011). Consistent with Long et al. (1991), we use the term "photoinhibition" to describe a potential drop in carbon assimilation caused by either photodamage or slow-reversing biochemical photoprotection. Aside from its direct effects, light can also alter other microclimatic factors, like temperature, soil moisture, and vapor pressure deficit (VPD), which can compound photoinhibition (Björkman & Powles 1984). For example, high VPD can lower carbon assimilation by causing stomatal closure, which reduces the potential to use light for photosynthesis; this effect, in turn, may increase the risk of photoinhibition, reducing photosynthetic capacity further. Competition may also may increase a plant's risk of photoinhibition if it reduces its access to resources in a way that limits photosynthesis. Thus, photodamage and photoprotective investments are likely to affect plants' fitness and distribution across environmental gradients (Külheim et al. 2002).

Given that light can cause stress, it may be possible for one plant species to facilitate another through shading. Whether shading by one species has a positive or negative overall effect on another depends on the balance of two effects:

1. Potential reduction of carbon gain through declines in light available for photosynthesis at any given instant; and,
2. Avoidance of chronic stress, which may increase photosynthetic rates at any given light level.

Monteith et al. (1977) defined light-use efficiency (LUE) as net photosynthesis divided by the amount of photosynthetically active radiation (PAR) absorbed. In terms of this formalism, an individual plant will have higher photosynthetic rates in the shade when the proportional benefit of (2) is greater than the proportional loss caused by (1). Changes in instantaneous irradiance alter the position along a photosynthetic light-response curve; changes in LUE alter the parameters of the curve such that plants assimilate more or less carbon at a given irradiance (Fig. 1).

Here, we test whether the shade created by trees can facilitate the carbon assimilation and growth of neighboring trees in a biodiversity experiment. Experimental and observational research alike has shown that biodiversity often promotes ecosystem functions such as productivity (Tilman et al. 2014). In forests, this trend has been shown through both experimental (Potvin & Gotelli 2008; Tobner et al. 2016; Grossman et al. 2017; Williams et al. 2017; Huang et al. 2018; Zemp et al. 2019) and observational (Gamfeldt et al. 2013; Liang et al. 2016; Oehri et al. 2017) data, across temperate (Tobner et al. 2016; Grossman et al. 2017; Williams et al. 2017), subtropical (Huang et al. 2018), and tropical (Potvin & Gotelli 2008; Zemp et al. 2019) forests. These positive relationships are robust to variation in climate, successional stage, and other factors (reviewed in Grossman et al. 2018; Ammer 2018).

One of the many factors that could contribute to positive biodiversity-productivity relationships is interspecific facilitation through reduction of abiotic stress (Wright et al. 2017). Some research has marshaled indirect evidence that facilitative interactions promote these relationships by linking patterns of productivity to species traits (Fichtner et al. 2017). Nevertheless, the physiological mechanisms that underlie these effects are poorly understood, despite their potential relevance for projecting species interactions under environmental change.

In this paper, we examined the interactions among tree species in the Forests and Biodiversity (FAB) experiment at Cedar Creek Ecosystem Science Reserve (East Bethel, MN). We ask: Do certain species aid the growth of others by shielding them from stresses caused by high irradiance? In particular, given that conifer species had higher initial growth rates (Table 1), we focused on whether they could facilitate the growth of broadleaf species through shading.

We addressed this question by measuring the physiology of carbon gain among broadleaf species across neighborhood environments. We examined whether photosynthetic physiology might explain patterns in aboveground woody growth. If shading by neighbors does have a net positive effect for some species, we would expect larger neighbors to cause focal individuals to have higher growth and carbon assimilation rates. We also posed the hypothesis that trees exposed to high light would use structural and biochemical photoprotective mechanisms more than those in lower light environments. If true, this

finding would imply that trees growing in high light must invest in photoprotection to avoid damage, reinforcing our proposition that light stress influences the interactions within these communities.

Methods

Experimental design

The Forests and Biodiversity (FAB) experiment began in 2013 and comprises 142 4 × 4 m plots, each planted with 64 trees in a 0.5 × 0.5 m grid. These plots form three blocks, each with 49 plots arranged in a 7 × 7 square. Neighboring plots within blocks are immediately adjacent to one another. Each plot is planted with 1, 2, 5, or 12 species from a pool of 12 total species (Table 1). These species include four evergreen conifers with needle-like leaves (two distinct families) and eight deciduous, broadleaf angiosperms (four distinct families). Except for five-species plots, each distinct species composition has a replicate in each block. All species in a plot have approximately equal frequency, and the placement of species within a plot is random. Further details about the experimental design can be found in Grossman et al. (2017).

The mean relative growth rate in monoculture during the first three years varied dramatically among species, being highest in conifers and *B. papyrifera* (Table 1). During these first three years, Grossman et al. (2017) found that diverse plots overyield in productivity—their growth is greater than a weighted average of the constituent species' growth in monoculture. Using the partition of Loreau & Hector (2001), most of this overyielding was due to complementarity effects, which are often interpreted as a result of synergistic interactions among species, rather than selection effects.

Tree growth

We surveyed tree growth in late fall of each year. For all living trees, we measured diameter and height to the tallest leader. We measured basal diameter (5 cm from the ground) for trees less than 137 cm tall; and diameter at breast height for trees more than 137 cm tall. For a subset of individuals, we measured both diameters. To predict basal diameter when it was not measured, we used linear

relationships predicting basal diameter from the height of the same individual in the same year and the basal diameter in the previous year.

We estimated woody stem volume as $V = \pi r^2 h$, where h is height and r is the basal radius (half the basal diameter). This assumes each tree stem is a cylinder, an assumption that has been used and justified in other tree diversity studies (Tobner et al. 2016; Williams et al. 2017), in the absence of system-specific allometric equations. We then calculated the yearly relative growth rate (RGR) between 2016 and 2018 as $RGR = (\ln V_{2018} - \ln V_{2016})/2$ (Hoffman & Poorter 2002). We chose 2016 as a starting point because no replanting of dead trees occurred after that point.

For each tree, we also calculated the average stem volume of its eight neighbors (in cardinal and intercardinal directions) in 2018 as a proxy for the intensity of aboveground interactions. We assessed neighbor effects on focal individual growth using ordinary least-squares (OLS) regression. When a neighbor was missing, either due to mortality or because the focal individual was on the edge of the experiment, we assigned that neighbor a volume of zero.

Photosynthetic physiology

We measured dark- and light-acclimated chlorophyll fluorescence parameters and reflectance spectra across all eight broadleaf species. We also measured photosynthetic light-response curves across four focal species (*A. rubrum*, *B. papyrifera*, *Q. ellipsoidalis*, and *T. americana*).

For measurements of physiology, we focused on three kinds of plots: (1) monocultures of broadleaf species ("monoculture"); (2) bicultures comprising one broadleaf and one conifer species ("shaded biculture"); and (3) twelve-species plots ("twelve-species") (see Fig. S1 for sample images). For each species in each treatment, we measured physiological parameters on six individuals—two in each of three plots. Neither *A. negundo* nor *Q. macrocarpa* was planted with a conifer in any biculture plots. We used *B. papyrifera* as a shaded biculture partner for *Q. macrocarpa* because it is a fast-growing species that draws down light availability. We omitted the shaded biculture treatment for *A. negundo*.

Photosynthetic light-response curves

We measured photosynthetic-light response curves from the four focal species during July 2018 using an LI-6400 gas exchange system (LI-COR BioSciences, Lincoln, NE) with a 6400-40 Leaf Chamber Fluorometer head. From each tree (n = 72 total), we selected a fully expanded upper leaf with no visible sign of disease or herbivory. We noted the angle of each leaf relative to horizontal to the nearest 15˚ before beginning measurements. Each curve had nine steps in descending order of brightness: 2000, 1500, 1000, 500, 200, 100, 50, 20, and 0 µmol m^{-2} s^{-1}. We also measured relative electron transport rate (ETR) using chlorophyll fluorescence at each light level. We maintained favorable conditions inside the chamber during each measurement. Following each curve, we removed the leaf to measure leaf mass per area (LMA). Further details about light-response curve procedures and ETR calculations can be found in the Supplemental Methods. Finally, we fitted a non-rectangular hyperbolic model (Lobo et al. 2013) to each light-response curve using *R* code written by Nick Tomeo, available at: https://github.com/Tomeopaste/AQ_curves.

We aimed to determine how carbon assimilation rates vary with the ambient light level, which we define as the photosynthetic photon flux density (PPFD) one might measure in an open field adjacent to the experiment. For most leaves we measured, *in situ* light availability is lower than the ambient light level, mainly because each tree is shaded by its neighbors. To estimate each tree's carbon assimilation as a function of ambient light, we have to transform its measured photosynthetic light-response curve along the *x*-axis according to its light availability.

For example, if the topmost leaves of a particular tree only receive 50% of ambient light, we would stretch its light-response curve two-fold along the *x*-axis. For this tree, the realized assimilation rate we estimate at an ambient (or open-field) PPFD of 2000 µmol photons m^{-2} s^{-1} would be the assimilation rate at an leaf-level PPFD of 1000 µmol m^{-2} s^{-1}. The exact scaling factor is estimated for each individual as $RLA \times \cos(\theta)$, where RLA is relative light availability (see *Light availability*) and θ is the leaf angle. (Taking the cosine of θ approximately corrects for the reduction in horizontally projected leaf area in steeply inclined leaves when the sun is directly overhead, as simplified from Ehleringer &

Werk [1986].) We used this procedure on each fitted curve in order to compare across treatments in a way that accounts for the variable light intensity each individual receives. We refer to photosynthetic light-response curves that describe a function of the leaf chamber PPFD as *chamber light-response curves*, and the rescaled light-response curves as a function of ambient PPFD as *ambient light-response curves*.

Finally, we used ambient light-response curves to estimate carbon assimilation by top leaves throughout July. We used an hourly averaged time series of ambient solar radiation from Carlos Avery Wildlife Management Area in Columbus, MN, 13.6 km away from the study site. Following Carruthers et al. (2001), we assumed a conversion of 0.217 μmol photons m^{-2} s^{-1} of PAR per Watt m^{-2} of solar radiation. By using these data as inputs to the ambient light-response curves, we could estimate integrated carbon assimilation across the month of July. This procedure assumes that the photosynthetic response to light remains constant, and is not affected by factors like leaf temperature and stomatal closure. This assumption is unrealistic, but we nevertheless consider it a useful way of estimating the consequences of realistic fluctuations in the light environment. We compared treatments within species using ANOVA.

Throughout the paper, we express assimilation per unit of leaf dry mass because we aim to determine the plants' return on investment in biomass. As expected, leaves growing in low light environments tended to have lower LMA in most species (Poorter et al. 2019), and expressing data on a mass basis accounts for these large differences in construction cost. We also express stomatal conductance (g_s) and electron transport rate (ETR) on a mass basis for comparison with assimilation rates, with the caveat that both of these processes typically occur near the leaf surface.

Instantaneous chlorophyll fluorescence, pigments, and spectral reflectance

Across all eight broadleaf species, we measured chlorophyll fluorescence parameters using an FMS2 pulse-modulated fluorometer (Hansatech Instruments Ltd., Norfolk, UK) over two days in late July (n = 138 total). We measured both dark- and light-acclimated parameters at the same spot on the same leaves. For dark-acclimation, we placed opaque leaf clips on the leaf the evening before measurement.

We then measured F_v/F_m within two hours after sunrise; this parameter is a general index of photoinhibition (including sustained photoprotection).

We took light-acclimated measurements between 12:00 and 14:00 each day. The protocol involved the following steps: actinic light at 1000 µmol m^{-2} s^{-1} for 15 seconds, a saturating pulse, and two seconds of far-red light. We exposed all leaves to the same actinic light because we aimed to assess photoprotective capacity under comparable light conditions, even though individual trees had different light environments.

From these data, we estimated qN, a parameter that indicates the extent of non-photochemical quenching under the imposed actinic light; this parameter is correlated with de-epoxidation of xanthophyll cycle pigments (Watling et al. 1997; Cavender-Bares and Bazzaz 2004). Following Kramer et al. (2004), we also calculated the quantum yields ϕ_{PSII}, ϕ_{NPQ}, and ϕ_{NO}, which sum to 1. These three parameters are the proportions of light energy dissipated through photochemistry, non-photochemical quenching, and non-regulated energy dissipation, respectively. The last is a crucial parameter because it represents the inability of a plant to dissipate light in a safe way; this portion of the absorbed light may contribute to photodamage. The Supplemental Methods contain formulas for all parameters and justifications for our choices in data analysis.

On separate top leaves of the same trees, we measured reflectance spectra (350-2500 nm) using a PSR+ 3500 field spectroradiometer (Spectral Evolution, Lawrence, MA). We used these spectra to calculate the photochemical reflectance index (PRI), a two-band index that most strongly indicates carotenoid : chlorophyll ratios (Gamon et al. 1992; Wong & Gamon 2015; Gitelson et al. 2017). This index is calculated as PRI = $(R_{531} - R_{570}) / (R_{531} + R_{570})$, where R_n is reflectance at a wavelength of *n* nm. Low PRI tends to indicate high carotenoid : chlorophyll ratios. We estimated species-specific OLS regression slopes of PRI and of each chlorophyll fluorescence parameter against relative light availability (see *Light availability*).

To understand how photoprotective allocation varies with adaptations to shade, we used shade tolerance values compiled by Niinemets & Valladares (2006) on a five-point scale based on prior literature. Higher values along this scale indicate that plants are able to grow in lower light conditions.

Phenology

We also monitored the timing of leaf abscission in monoculture and shaded biculture plots for *T. americana* to assess whether shade could delay senescence and abscission, extending the period for carbon gain (Cavender-Bares et al. 2000). In early August, we surveyed 120 *T. americana* trees (60 in monoculture, 60 in shaded biculture) to determine the proportion of leaves that had fallen based on how many of the top five axillary buds lacked a leaf. From each of these trees, we marked a single leaf and returned every 1-2 weeks to monitor its senescence. We assessed each leaf on a binary basis (senesced or not) based on whether it had at least 50% remaining green leaf area. We chose this criterion as a simple proxy for the continuous scale used by Cavender-Bares et al. (2000). Based on the initial survey and the repeated surveys of marked leaves, we tracked the proportion of leaves that had senesced over time. To ensure that leaves were photosynthetically active until near the point of senescence, we collected a one-time measurement of dark-acclimated F_v/F_m in mid-September among remaining leaves.

We also performed a one-time measurement of 60 (30 per treatment) *A. rubrum* plants on October 1, using the same protocol we used to do our initial early August survey of *T. americana*. We aimed for this survey to help test the validity of our results across species.

Water potential

Water deficits—even moderate ones—can reduce carbon gain by causing stomata to close (Brodribb et al. 2003). To assess how our treatments affected water status, we measured leaf water potential using a Scholander pressure bomb. We measured pre-dawn water potential (Ψ_{PD}) in all eight broadleaf species (n = 96) and midday water potential (Ψ_{MD}; between 12:00 and 14:00) in only the four focal species (n = 48). In these measurements, we included monoculture and shaded biculture treatments,

except in *A. negundo*, where we used the twelve-species treatment in place of the absent shaded biculture treatment. For all water potential measurements, we removed leaves and immediately placed them in impermeable plastic bags with wet paper towels, which we stored in a cooler. We then transported leaves indoors to be measured within 90 minutes.

Because we only intended to test whether there was a general tendency, across species, for water potential to vary with treatment, we included species identity as a random effect and treatment as a fixed effect in both models.

Leaf angles

Leaf angle is a key control on light exposure because more vertical leaves intercept less light when the sun is directly overhead, and allow light to percolate deeper into the canopy. As a result, steep leaf angles can be a key structural strategy for avoiding light, temperature, and water stress (Valladares & Pugnaire 1999; Werner et al. 1999; Pastenes et al. 2004; Valiente-Banuet et al. 2010). We predicted that trees in monoculture would have steeper leaf angles than those in other treatments because they need to avoid excess light. From each of three species (*A. rubrum*, *Q. ellipsoidalis*, and *T. americana*), we randomly selected five individuals from each of six plots—three from monoculture treatments, three from shaded bicultures (n = 15 per species × treatment). On these individuals, we measured the leaf angle from horizontal, to the nearest 15˚, of the top five leaves in the crown.

Because angles of leaves within individuals may be non-independent, we tested differences among treatments using a mixed-effects model with treatment as a fixed effect and individual tree nested within plot as a random effect. Because deviations from horizontal in either direction can reduce light interception, we used the absolute value of leaf angle as the dependent variable in statistical analyses. We calculated p-values using Satterthwaite's degrees of freedom method in the *lmerTest* package (Kuznetsova et al. 2017), with the caveat that such values should be interpreted conservatively.

Environmental data

Light availability

On a cloudy day, under diffuse light conditions, we measured light interception above each tree selected for this study (n = 138) using an AccuPAR LP-80 ceptometer (METER Group, Pullman, WA). We took the mean of two to four PAR measurements in the open and the mean of two measurements directly above the topmost leaf of each tree. By calculating a ratio of these values, we could calculate the percent of light transmitted to the top of each tree. We called this value *relative light availability*. This value is typically well-correlated with the percentage of ambient light available over much longer time-scales (Parent & Messier 1996).

Soil water content

We collected a one-time measurement of soil volumetric water content in mid-August using a FieldScout Time-Domain Reflectometer 350 (Spectrum Technologies, Inc., Aurora, IL). This single measurement followed six days from the last major rain. At midday, we collected and averaged three measurements in each of 32 plots, spanning monocultures of the four core broadleaf species, shaded bicultures, and twelve-species plots.

Air temperature

For nine days during early September, we set out four Thermochron iButtons (model DS1921G; Maxim Integrated Products, Sunnyvale, CA, USA) in shaded plots and two in twelve-species plots, setting them to log air temperature hourly. Each iButton was suspended on mesh inside a 1 m-tall PVC pipe that was capped with an elbow to shield against solar irradiance. We compared these data to air temperature measured hourly under open, sunny conditions at the Cedar Creek LTER weather station about 0.77 km away. We assumed that data from this station would be representative of air temperature in

non-shaded areas. We ignored nighttime and early morning (20:00-08:00 h) readings because iButtons may have been influenced by evaporative cooling of condensed water droplets.

Results

Tree size and growth

Neighborhood-scale relationships between focal individual RGR and total neighbor stem volume were noisy but highly significant in most species (Fig. 2). The sign and strength of the relationships varied among species. In most species, individuals with larger neighbors had lower RGR, including in *A. rubrum* (R^2 = 0.033, p <10^{-5}), *Q. alba* (R^2 = 0.038, p <10^{-6}), *Q. ellipsoidalis* (R^2 = 0.030, p <10^{-5}), *Q. macrocarpa* (R^2 = 0.027, p <10^{-5}), and *Q. rubra* (R^2 = 0.056, p <10^{-9}). On the other hand, some species grew faster with larger neighbors, including *A. negundo* (R^2 = 0.018, p < 0.005) and *T. americana* (R^2 = 0.019, p <10^{-4}). *B. papyrifera* showed no significant relationship with neighbor size. These results are qualitatively unchanged by eliminating trees on the edge of the experiment or incorporating plot as a random effect.

Although these individual-level effects are noisy, they show strong tendencies in average stem growth across the full range of potential neighbor size. Imagine two *T. americana* trees that begin at the same size in 2016: One in monoculture, where the average neighbor in 2018 is 573 cm^3, and one growing in a shaded biculture with *Pinus strobus*, where the average neighbor is 2175 cm^3. The neighborhood-level regression predicts that after two years, the average *T. americana* in the shaded biculture would be 39.7% larger due to the difference in RGR. Or, consider *Q. rubra*, which had the strongest negative response to neighbor size: We predict that an average tree in the shaded biculture would be 39.1% smaller than in monoculture. Because these figures assume that treatments show no average size differences by 2016, they may underrepresent the true differences in size that have accumulated and may continue to accumulate with time.

We can also aggregate these observations to the plot scale—for example, by considering the RGR of summed stem volume of each species in each plot (Fig. 2). (This approach is distinct from an average

of individual RGRs, which assigns equal weight to small and large individuals.) Although aggregation leaves less power to detect significant relationships, the relationships we find here explain much more of the variation in growth across plots, including negative RGR responses to average neighbor biomass in *Q. alba* (R^2 = 0.311, $p < 0.001$) and *Q. macrocarpa* (R^2 = 0.174, $p < 0.01$) and a positive response in *T. americana* (R^2 = 0.282, $p < 0.001$).

Trees that died between 2016 and 2018 dropped out of our individual-level analyses of RGR because their stem volume was 0 in 2018, making it impossible to calculate RGR. To see whether mortality could alter our conclusions, we also performed statistical analyses on untransformed growth in stem volume from 2017 to 2018, in which we alternately (1) treated mortality as a decline in volume to 0, or (2) removed trees that died from analyses. The rate of mortality was low between 2016 and 2018 (~7.5%), and accounting for mortality makes no qualitative difference when considering absolute growth as the response variable (Fig. S2).

Photosynthetic physiology

Photosynthetic light-response curves

In three out of the four focal species (*Q. ellipsoidalis*, *A. rubrum*, and *T. americana*), photosynthetic rates (per unit dry mass) were higher in shaded biculture and twelve-species treatments than in monoculture at any given chamber light level (Fig. 3, left). In the lone pioneer species, *B. papyrifera*, photosynthetic rates in shaded biculture were lower than in the other two treatments.

The rate of photosynthesis is often limited by either ETR or by RuBP carboxylation rate, which in turn is often limited by stomatal diffusion of CO_2 (Farquhar et al. 1980). In our data, both ETR and stomatal conductance (g_s) increase with light availability (Fig. S3). (ETR tends to decline at very high light levels, especially in shaded treatments, perhaps due to acute photoinhibition.) Within each species, the rank-order of treatments in photosynthetic rates, ETR, and g_s tend to be broadly congruent. One exception is that *T. americana* in shaded biculture has much higher g_s than in twelve-species or monoculture plots, despite having slightly lower photosynthetic rates than in twelve-species plots.

Compared to chamber light-response curves, the picture that emerges from ambient light-response curves is more complex (Fig. 3, right). In *B. papyrifera*, the shaded biculture treatment still had the lowest assimilation rate across light levels. In late-successional *T. americana*, the shaded biculture and twelve-species treatments had higher assimilation rates across most light levels, by up to 25%. In the other two species, assimilation rates were highest in monoculture at low light availability; as top-of-canopy light increases, assimilation rates for twelve-species and (in *Q. ellipsoidalis*) shaded biculture plots eventually intersect and surpass monoculture rates.

Using a time series of solar radiation, we estimated total assimilation rates in July 2018 based on each ambient light-response curve (Fig. S4). We found that trees would have lower total assimilation in shaded biculture than in monoculture in *A. rubrum* (ANOVA; $p = 0.012$) and *B. papyrifera* ($p = 0.003$); in both species, trees in twelve-species plots did not differ from those in monoculture. In the other two focal species, there were no significant differences among treatments. In these integrated estimates, the costs of shade seem larger than one might suppose from looking only at instantaneous assimilation rates under high ambient light. We attribute these high costs to the fact that light levels were frequently low; PPFD was under 500 μmol m^{-2} s^{-1} more than 60% of the time. It is under these low-light conditions that trees in monoculture most outperform those in shaded biculture.

Instantaneous chlorophyll fluorescence, pigments, and spectral reflectance

Among all eight species except the early-successional *B. papyrifera*, dark-acclimated F_v/F_m declined as relative light availability increased (Fig. 4), showing that high light exposure causes photoinhibition. Across all trees of the four focal species, dark-acclimated F_v/F_m is positively correlated with light-saturated photosynthetic rates (A_{sat}), as estimated from the non-rectangular hyperbolic model (OLS regression; $R^2 = 0.44$; $p < 10^{-9}$; Fig. 5). Slopes are not significantly different among species. This effect suggests that photoinhibitory declines in PSII efficiency may contribute to variation in light-response curves.

In most species, qN rose with *in situ* light availability, indicating that trees that grow in high light have a higher capacity to dissipate excess light with non-photochemical quenching (Fig. 4). However, two species were clear exceptions: In *T. americana* and *A. negundo*, qN was nearly invariant across the range of light availability they experienced, which suggests that these species are unable to upregulate photoprotection in full sun.

Extracting the species-specific slopes of the change in dark-acclimated F_v/F_m with relative light availability, we find that that the species with the greatest decline in F_v/F_m are the most shade-tolerant (Fig. 5; $R^2 = 0.601$; $p = 0.025$). Similarly, more shade-tolerant species have less (or no) increase in qN at high light availability ($R^2 = 0.619$; $p = 0.022$). These results suggest that shade-tolerant species may fail to protect themselves from excess light when growing in light-saturated environments, making them susceptible to photoinhibition. This suggestion is borne out in patterns of ϕ_{NO} across light environments, which show that *T. americana* and *A. negundo* exposed to 1000 μmol photons m^{-2} s^{-1} are just as susceptible to non-regulated dissipation of light when growing in full sun as in the shade (Fig. 4).

On a ternary plot, we plotted ϕ_{PSII}, ϕ_{NPQ}, and ϕ_{NO}—the quantum yields of PSII photochemistry, non-photochemical quenching, and non-regulated dissipation, respectively—to illustrate how light energy is dissipated differently across treatments (Fig. S5). Our results broadly show that across species, when exposed to an equivalent, high level of light per unit area, trees that develop in the sun vary in ϕ_{PSII} and ϕ_{NPQ} but have lower ϕ_{NO}. However, because they regularly experience higher light levels, they may still be at high risk of damage.

PRI declined with increasing light availability in all species, which supports the idea that trees in monoculture allocate more to carotenoids (Fig. 4). Although this relationship had remarkably consistent slopes and intercepts across nearly all species, *B. papyrifera* had higher PRI at all light levels within its narrow domain.

Phenology

In *T. americana*, leaf abscission in monoculture began in early August, and more than half of all leaves had senesced by September 3 (Fig. 6). In shaded bicultures, more than 90% of leaves remained by September 3, and no survey found greater than 50% senescence until October 1. We assigned the senescence date of each leaf as the date of the first survey by which it had senesced; using this response variable, leaves in monoculture senesced much earlier than those in shaded cultures (t-test; $p < 10^{-11}$). These results suggest that leaves in shaded bicultures had, on average, one additional month for carbon gain. Here, we assume that leaves in shaded biculture did not downregulate photosynthesis long before abscission, which was supported by mid-September measurements of dark-acclimated F_v/F_m. In shaded biculture, dark-acclimated F_v/F_m averaged 0.745 at this point, which was higher than the mean among remaining monoculture leaves, 0.642 (t-test; $p = 0.061$).

Our one-time measurement of *A. rubrum* leaves in early October suggested that this pattern is not limited to *T. americana*. *A. rubrum* trees in shaded biculture plots retained about 56% of their leaves, while those in monoculture retained only 10% (t-test; $p < 10^{-4}$).

Water potential

For Ψ_{PD}, we removed two data points—one in shaded biculture, one in monoculture—with values more negative than -0.8 MPa on the grounds that they may have been caused by measurement error. Across treatments, the mean Ψ_{PD} and Ψ_{MD} were -0.15 and -1.29 MPa, respectively. Ψ_{PD} in shaded bicultures was more negative than in monocultures by about 0.07 MPa ($p = 0.004$). This result holds even when including the outliers ($p = 0.049$), with a mean difference of 0.08 MPa between treatments (Fig. S6). By midday, this pattern reversed; Ψ_{MD} was more negative in monocultures than shaded bicultures, with a mean difference of 0.33 MPa ($p = 0.004$).

Leaf angles

Among each of the three species in which we measured leaf angles, leaves were more horizontal in the shaded biculture treatment (Fig. 7). The size of this effect varied among species: 9.0˚ in *Q. ellipsoidalis* ($p = 0.037$), 22.0˚ in *A. rubrum* ($p = 0.022$), and 25.0˚ in *T. americana* ($p = 0.002$). The direction of this shift varied among species. Because *T. americana* leaves usually drooped downward in monoculture, leaf angles became less negative in shade. In contrast, *Q. ellipsoidalis*, whose leaves were often inclined upwards in monoculture, had less positive leaf angles in the shade. In *A. rubrum*, leaf angles in monoculture were inclined both up and down, while in shade, leaves had a tendency to become more horizontal.

Environmental factors

In our survey, soil moisture varied among treatments (ANOVA; $p < 0.01$); it was lowest (5.7%) in shaded biculture plots and highest (7.2%) in broadleaf monoculture plots. We found that daytime air temperature in the open was higher than in shaded bicultures or twelve-species plots at 62.5% of hourly log-points during the nine-day logging period. The air temperature in monocultures averaged 1.03˚ C higher over this period.

Discussion

We investigated how species interactions in a tree diversity experiment might emerge from the physiological responses of trees to the light environment created by their neighbors. We found that two species (*A. negundo*, *T. americana*) grew faster on average with larger neighbors, while five (*A. rubrum*, *Q. alba*, *Q. ellipsoidalis*, *Q. macrocarpa*, and *Q. rubra*) grew slower. The two species with positive responses to neighbor size were shade-tolerant and faced a high risk of photoinhibition in high light, which could cause carbon assimilation to be lower in monoculture. In contrast, the five species with negative responses increased non-photochemical quenching in high light and tended to have lower carbon gain in shaded bicultures. These results suggest that the divergent responses of these two groups of

species were driven, at least in part, by their tolerance to excess light. Here, we interpret these patterns in further detail.

Physiology of carbon gain

We chose our four focal species along a gradient from early-successional, shade-intolerant *B. papyrifera*, to mid-successional *A. rubrum* and *Q. ellipsoidalis*, to late-successional, shade-tolerant *T. americana* (Braun 1954). This successional gradient aligns with the varied consequences of shade for carbon gain across species. Growing in a shaded biculture can either: (1) decrease assimilation rates (compared to monoculture) at all ambient light levels, as in *B. papyrifera*; (2) decrease assimilation under low ambient light, but increase it under high light, as in *A. rubrum* and *Q. ellipsoidalis*; or (3) increase assimilation rates at nearly all ambient light levels, as in *T. americana*. Our finding that carbon gain in *T. americana* increases under shade is reinforced by Carter and Cavaleri (2018), who find that its photosynthetic rates may increase down vertical gradients from the upper canopy to the sub-canopy.

The untransformed light-response curves can help us identify the causes of these patterns. As a function of leaf chamber PPFD—without penalizing for lowered light availability—three of our four species (*A. rubrum*, *Q. ellipsoidalis*, and *T. americana*) had higher photosynthetic rates in the shaded biculture and twelve-species treatments than in monoculture (Fig. 3, left). In all species except early-successional *B. papyrifera*, dark-acclimated F_v/F_m declines with light availability. Because dark-acclimated F_v/F_m correlates with A_{sat}, this result suggests a role for photoinhibition in determining photosynthetic rates. Because photoinhibition most often occurs through damage or regulation of PSII, it is usually thought to depress photosynthesis by lowering ETR. However, both ETR and stomatal conductance seem to reflect the patterns in photosynthesis across treatments in chamber light-response curves (Fig. S3), suggesting that both have some role in explaining why most species showed lower photosynthesis in monoculture.

Given that light availability fluctuates—diurnally, seasonally, and with cloud cover—the treatment that performs best may also vary from moment to moment. We produced a more integrated

picture by estimating total assimilation during the month of July, assuming that each tree's photosynthetic light-response curve remains constant (Fig. S4). While trees in shaded bicultures had lower estimated assimilation than in monoculture in two of our focal species (*B. papyrifera* and *A. rubrum*), those in twelve-species plots had similar assimilation compared to those in monoculture in all four species. It seems plausible that the intermediate light environment in these twelve-species plots allowed trees to avoid photoinhibition without becoming frequently light-limited. We caution that these measurements are only based on top leaves, such that we cannot directly evaluate whole-plant carbon gain.

These estimates of assimilation during July cannot explain certain features in our stem biomass data—including, for instance, the clearly positive effect of neighbor size on growth in *T. americana*. We next discuss two kinds of phenomena that could contribute to variation in growth rates, but which analyses based on light-response curves do not account for: Delayed senescence and microclimatic effects. Both may contribute to potential positive effects of shading by neighbors.

T. americana in shade dropped their leaves nearly a month later into the fall compared to in monoculture (Fig. 6). We also found accelerated senescence in full sun in *A. rubrum*. Given that most leaves remained photosynthetically active until shortly before abscission (as in Mattila et al. 2018), shade can allow plants a longer period of carbon gain. The pattern that the light environment affects senescence timing admits at least two explanations: (1) that plants in the sun accumulate phenological cues for senescence related to temperature, or (2) that excess light and other stresses cause damage that accelerates senescence (Cavender-Bares et al. 2000), especially as the temperature declines, rendering leaves more susceptible to photodamage (Juvany et al. 2013; Renner & Zohner 2019). Contrary to the first explanation, air temperatures in full sun remained higher than in shaded plots.

Although we emphasize the role of light stress, other microclimatic factors could contribute to variation in photosynthetic rates among treatments. Because we aimed to control the chamber microclimate during light-response curves, we may have excluded some effects of the ambient microclimate from our photosynthesis estimates. For example, midday leaf water potential tended to be somewhat more negative in monoculture—perhaps due to greater VPD—which could make stomata close

more often (Fig. S6). On the other hand, pre-dawn leaf water potential was slightly more negative in shaded bicultures, which may owe to lower soil moisture. Our water potential measurements show that water stress was not very severe in any treatment, but even modest differences could affect stomatal behavior (Brodribb et al. 2003). In addition, it seems plausible that greater light exposure may make leaf temperature higher in monoculture (Schymanski et al. 2013), which could push leaves above thermal optima for photosynthesis.

In summary, we contend that shade has both costs and benefits. Being shaded reduces the light available for photosynthesis, but it may also prevent chronic stress due to excess light, allowing the plant to use the light it absorbs more efficiently. Both factors must be jointly considered to determine whether shade benefits or harms a plant.

Interpreting patterns of stem growth

The stem growth data are consistent with the hypothesis that larger neighbors can facilitate growth in *T. americana* and *A. negundo*, the most shade-tolerant species. In light of the physiological data, we interpret this pattern as a result of abiotic stress amelioration. Because we lacked measures of root allocation, we cannot rule out the hypothesis that this trend is caused by a shade avoidance response that increases allocation to shoots compared to roots (Schall et al. 2012). Nevertheless, the idea that much of this effect is facilitative is supported both by the physiological data and by other studies that have found that shade can increase total (root and shoot) biomass (e.g. Ryser & Eek 2000; Semchenko et al. 2012).

In the majority of species, including all four *Quercus* species and *A. rubrum*, larger neighbor size caused focal individual size to be smaller, which we interpret as the result of net competitive interactions, potentially both aboveground and belowground. The occurrence of belowground competition is suggested by the fact that soil moisture was lowest in our dense-growing shaded biculture plots. *B. papyrifera*, a shade-intolerant early-successional species whose leaves had lower photosynthetic rates in the shaded biculture, had a neutral response to neighbor size, perhaps because its rapid height growth allowed it to

overtop neighbors rather than be overtopped. In contrast to all the other broadleaf species, its top leaves suffered no reduction of light availability in shaded biculture, compared to monoculture.

Mechanisms of photoprotection

Plants use multiple means to avoid damage from excess light, which can be classified broadly into biochemical and structural strategies. Our results show that trees in full sun allocate more to pigment-based methods of photoprotection, as shown by lower PRI, and higher qN in most species. The two most shade-tolerant species—*A. negundo* and *T. americana*—do not show a greater capacity for non-photochemical quenching when grown in full sun. Across a gradient of shade to sun, these species may experience large increases in ϕ_{NO}, and may suffer from greater photodamage as a result, as supported by patterns of dark-acclimated F_v/F_m. This result is consistent with other research that finds that shade-adapted species often fail to develop strong photoprotective abilities in the sun (Montgomery et al. 2008).

Our survey of leaf angles is also consistent with the idea that plants may steeply incline their leaves to avoid intercepting excess light—a form of structural photoprotection. Leaves that are steeply inclined tend to intercept less light per unit area, particularly during midday, when solar radiation is otherwise most intense. The dramatic trend we observe in leaf angles suggests that these species are able to use gross structural characteristics to partially regulate their light absorption.

Plants—especially those that grow in the shade—may lack perfect photoprotective mechanisms in part because they are costly. Building pigments and proteins for photoprotection uses nutrients that could otherwise be allocated to chlorophyll, RuBisCO, or structural tissue components. Furthermore, slow relaxation of NPQ may hinder photosynthesis even when periodic declines in light availability remove the immediate threat of damage (Zhu et al. 2004; Murchie & Niyogi 2011; Kromdijk et al. 2016). Steep leaf angles may also reduce carbon assimilation by reducing light interception even under low light. However, plants in full sun may need these mechanisms to avoid even greater long-term costs caused by photodamage. Our measurements of the mechanisms of photoprotection suggest that these species may

incur some risk of damage under high light, reinforcing our conclusions about the role of light stress in shaping species interactions.

The case for facilitation

An important result of our study is that shade from large neighbors increases both net photosynthetic rates and stem growth rates in shade-tolerant species. This finding has precedents: Ball et al. (1991) and Egerton et al. (2000) found that shade enhanced photosynthesis and growth of evergreen *Eucalyptus* seedlings during the winter, when cold temperatures impose a risk of photoinhibition. Howell et al. (2002) also found that the leafless outer branches of New Zealand's divaricating shrubs reduce photoinhibition by shading inner leaves.

Much of the work on facilitation in plant communities is guided by the stress-gradient hypothesis (SGH), which proposes that facilitative interactions are more common in stressful environments (Bertness & Callaway 1994; Maestre et al. 2009). We can understand photoinhibition in light of the SGH as follows: Stressful conditions limit the use of light for photochemistry, causing high light exposure to become a potential stressor. Under these conditions, shade from neighbors can ameliorate stress, causing facilitation. Under benign conditions, where plants can use more of the available light for photochemistry, high light exposure may not cause damage. Here, shading by neighbors can cause light limitation, resulting in an adverse, competitive effect on growth. As we show here, species' physiological traits also influence whether they are stressed by their environment.

Ever since the SGH was first described, the role of facilitative interactions in structuring plant communities has received more attention. For example, Bimler et al. (2018) suggest that models of species occurrence will be more accurate when they incorporate positive interactions. Nevertheless, the role of facilitation in structuring plant communities is still often overlooked (Wright et al. 2017), and its mechanisms are seldom assessed by measuring physiological rates (but see, for example, Barron-Gafford et al. 2017).

Competition and facilitation in biodiversity-ecosystem function relationships

Overyielding—or biodiversity-enhanced growth—is a hallmark of positive biodiversity-ecosystem function relationships. A whole community can only overyield if at least one of its constituent species overyields. Although we show how species growth changes with neighbor size, not neighbor diversity, our results show that shading allows some species to achieve greater biomass in shaded bicultures or twelve-species plots. In the same experiment, Grossman et al. (2017) found that *T. americana* has the greatest overyielding in multi-species plots of any broadleaf species, especially when growing with conifers or *B. papyrifera*. Grossman et al. (2017) further showed that conifer partners in these species combinations also grow faster than in monoculture, resulting in community overyielding.

In general, the species that faced the strongest negative effects from shade had physiological tolerance to high light and experienced shading as a form of competition. On the other hand, species that were facilitated by shade had low tolerance to excess light and likely benefited from the milder microclimate their neighbors created. We can place these findings in the context of the three classes of facilitative mechanisms distinguished by Wright et al. (2017):

1. Biotic facilitation, which is mediated by the activity of higher-order trophic interactions, such as promotion of shared mutualists or dilution of natural enemy loads;
2. Abiotic facilitation through resource enrichment, in which some species increase resource availability for others; and,
3. Abiotic facilitation through stress amelioration, in which some species create a favorable microclimate for others.

In the FAB experiment, enemy-mediated biotic facilitation is likely to have a limited role; Grossman et al. (2018) found that diversity had a mild influence on damage by herbivores and pathogens, and the direction of the relationship varied among tree species and herbivore guilds. Nutrient enrichment is unlikely to be a major mechanism for facilitation here because, although nitrogen is the main limiting mineral nutrient at Cedar Creek (Tilman 1987), none of the planted tree species associates with nitrogen-fixing microbes. As a result, stress amelioration is likely to be the main class of facilitation in this

experiment, perhaps acting in concert with niche partitioning and (to a limited extent) selection effects to drive overyielding.

In much of the literature on biodiversity and ecosystem function, the attempt to parse out explanations—such as niche partitioning and facilitation—often depends on ever-finer statistical partitions of biomass data (Loreau & Hector 2001; Fox & Kerr 2012), whose interpretation is often contested (Carroll et al. 2011; Pillai et al. 2019). Because the processes that drive biomass accumulation are ultimately physiological, physiological measurements can guide a mechanistic interpretation of biomass patterns. These techniques can help us determine what specific kinds of plant-plant and plant-environment interactions produce biodiversity-productivity relationships, and how these interactions emerge from basic aspects of plant function.

In this study, the survey-based biomass data and the physiological measurements generally converge in showing that certain species respond positively to the size of their neighbors, while others respond negatively. However, the physiological measurements allow us to reach a deeper level of explanation, showing how these interactions emerge in part from the photosynthetic responses of trees to the light environment created by their neighbors. Thus, we demonstrate that community ecology can benefit by incorporating mechanistic approaches from physiology.

Acknowledgements

We acknowledge that University of Minnesota, including Cedar Creek ESR, lies on the ancestral, traditional, and contemporary Land of the Dakota. This research was inspired in large part by conversations with Jake Grossman and Laura Williams. Beth Fallon, German Vargas G., Artur Stefanski, Daniel Stanton, and Danielle Way all gave valuable advice about measuring photosynthesis. Cathleen Nguyen and Chris Buyarski provided tremendous logistical support for data collection in FAB; Troy Mielke, Kally Worm, Jim Krueger, Pam Barnes, Mark Saxhaug, Dan Bahauddin, and others supported other crucial aspects of Cedar Creek infrastructure. Many Cedar Creek interns helped in the stem volume survey. Sarah Hobbie and Peter Reich contributed to the design of the FAB experiment. The Cavender-Bares lab (especially Gerard Sapès), Daniel Stanton, German Vargas G., Artur Stefanski, Jamie Mosel, José Lopez, and David Kramer all provided feedback on the results or manuscript. The FAB experiment is maintained with support from National Science Foundation under DEB #1234162 to Cedar Creek LTER. Spectral measurements were conducted as part of NSF/NASA DEB #1342778 to J.C.B. and R.M.. S.K. has been supported by an NSF Graduate Research Fellowship (Grant No. 00039202) and a UMN Doctoral Dissertation Fellowship. R.M. is also supported by Minnesota Agricultural Experiment Station project MIN-42-060.

References

Ammer C. Diversity and forest productivity in a changing climate. New Phytologist 221, 50–66 (2019).

Ball MC, Hodges VS, Laughlin GP. Cold-Induced Photoinhibition Limits Regeneration of Snow Gum at Tree-Line. Functional Ecology 5, 663–668 (1991).

Barron-Gafford GA, Sanchez-Cañete EP, Minor RL, Hendryx SM, Lee E, Sutter LF, Tran N, Parra E, Colella T, Murphy PC et al. Impacts of hydraulic redistribution on grass–tree competition vs facilitation in a semi-arid savanna. New Phytologist 215, 1451–1461 (2017).

Bertness MD, Callaway R. Positive interactions in communities. Trends in Ecology & Evolution 9, 191–193 (1994).

Bimler MD, Stouffer DB, Lai HR, Mayfield MM. Accurate predictions of coexistence in natural systems require the inclusion of facilitative interactions and environmental dependency. Journal of Ecology 106, 1839–1852 (2018).

Björkman O, Powles SB. Inhibition of photosynthetic reactions under water stress: interaction with light level. Planta 161, 490–504 (1984).

Braun-Blanquet J. Plant Sociology (trans. Fuller GD, Conard HS). New York: McGraw-Hill (1932).

Brodribb TJ, Holbrook NM, Edwards EJ, Gutiérrez MV. Relations between stomatal closure, leaf turgor and xylem vulnerability in eight tropical dry forest trees. Plant, Cell & Environment 26, 443–450 (2003).

Canham CD, Finzi AC, Pacala SW, Burbank DH. Causes and consequences of resource heterogeneity in forests: interspecific variation in light transmission by canopy trees. Can. J. For. Res. 24, 337–349 (1994).

Carroll IT, Cardinale BJ, Nisbet RM. Niche and fitness differences relate the maintenance of diversity to ecosystem function. Ecology 92, 1157–1165 (2011).

Cavender-Bares J. Chilling and freezing stress in live oaks (Quercus section Virentes): Intra- and interspecific variation in PS II sensitivity corresponds to latitude of origin. Photosynthesis Research 94, 437–453 (2007).

Cavender-Bares J, Bazzaz FA. From Leaves to Ecosystems: Assessing Photosynthesis and Plant Function in Ecological Studies. In Papageorgiou GC and Govindjee (Eds.), Chlorophyll fluorescence: A Signature of Photosynthesis (pp. 737–755). Dordrecht, Netherlands: Kluwer Academic Publishers (2004).

Cavender-Bares J, Potts M, Zacharias E, Bazzaz FA. Consequences of CO2 and light interactions for leaf phenology, growth, and senescence in Quercus rubra. Global Change Biology 6, 877–887 (2000).

Demmig-Adams B, Adams, WW III. Photoprotection and Other Responses of Plants to High Light Stress. Annual Review of Plant Physiology and Plant Molecular Biology 43, 599–626 (1992).

Demmig-Adams B, Adams, WW III. An integrative approach to photoinhibition and photoprotection of photosynthesis. Environmental and Experimental Botany 154, 1–3 (2018).

Dybzinski R, Tilman D. Resource Use Patterns Predict Long-Term Outcomes of Plant Competition for Nutrients and Light. The American Naturalist 170, 305–318 (2007).

Egerton JJG, Banks JCG, Gibson A, Cunningham RB, Ball MC. Facilitation of Seedling Establishment: Reduction in Irradiance Enhances Winter Growth of *Eucalyptus pauciflora*. Ecology 81, 1437–1449 (2000).

Ehleringer J, Werk KS. Modifications of solar radiation absorption patterns and the implications for carbon gain at the leaf level. In T. Givnish (ed.), On the Economy of Plant Form and Function. Cambridge Univ. Press, London. 57-82 (1986).

Farquhar GD, von Caemmerer S, Berry JA. A biochemical model of photosynthetic CO_2 assimilation in leaves of C_3 species. Planta 149, 78–90 (1980).

Fichtner A, Härdtle W, Li Y, Bruelheide H, Kunz M, von Oheimb G. From competition to facilitation: how tree species respond to neighbourhood diversity. Ecology Letters 20, 892–900 (2017).

Fox JW, Kerr B. Analyzing the effects of species gain and loss on ecosystem function using the extended Price equation partition. Oikos 121, 290–298 (2012).

Gamfeldt L, Snäll T, Bagchi T, Jonsson M, Gustafsson L, Kjellander P, Ruiz-Jaen MC, Fröberg M, Stendahl J, Philipson CD et al. Higher levels of multiple ecosystem services are found in forests with more tree species. Nature Communications 4, 1340 (2013).

Gamon JA, Peñuelas J, Field CB. A narrow-waveband spectral index that tracks diurnal changes in photosynthetic efficiency. Remote Sensing of Environment 41, 35–44 (1992).

Gitelson AA, Gamon JA, Solovchenko, A. Multiple drivers of seasonal change in PRI: Implications for photosynthesis 1. Leaf level. Remote Sensing of Environment 191, 110–116 (2017).

Grossman JJ, Cavender-Bares J, Reich PB, Montgomery RA, Hobbie SE. Neighborhood diversity simultaneously increased and decreased susceptibility to contrasting herbivores in an early stage forest diversity experiment. Journal of Ecology 107, 1492–1505 (2019).

Grossman JJ, Vanhellemont M, Barsoum N, Bauhus J, Bruelheide H, Castagneyrol B, Cavender-Bares J, Eisenhauer N, Ferlian O, Gravel D et al. Synthesis and future research directions linking tree diversity to growth, survival, and damage in a global network of tree diversity experiments. Environmental and Experimental Botany 152, 68–89 (2018).

Hoffmann WA, Poorter H. Avoiding Bias in Calculations of Relative Growth Rate. Annals of Botany 90, 37 (2002).

Howell CJ, Kelly D, Turnbull MH. Moa ghosts exorcised? New Zealand's divaricate shrubs avoid photoinhibition. Functional Ecology 16, 232–240 (2002).

Huang Y, Chen Y, Castro-Izaguirre N, Baruffol M, Brezzi M, Lang A, Li Y, Härdtle W, von Oheimb G, Yang V et al. Impacts of species richness on productivity in a large-scale subtropical forest experiment. Science 362, 80–83 (2018).

Juvany M, Müller M, Munné-Bosch S. Photo-oxidative stress in emerging and senescing leaves: a mirror image? J Exp Bot 64, 3087–3098 (2013).

Kothari S, Cavender-Bares J, Bitan K, Verhoeven AS, Wang R, Montgomery RA, Gamon J. Community-wide consequences of variation in photoprotective physiology among prairie plants. Photosynthetica 56, 455–467 (2018).

Kramer DM, Johnson G, Kiirats O, Edwards GE. New Fluorescence Parameters for the Determination of QA Redox State and Excitation Energy Fluxes. Photosynthesis Research 79, 209–218 (2004).

Kromdijk J, Głowacka K, Leonelli L, Gabilly ST, Iwai M, Niyogi KK, Long SP. Improving photosynthesis and crop productivity by accelerating recovery from photoprotection. Science 354, 857–861 (2016).

Külheim C, Ågren J, Jansson S. Rapid Regulation of Light Harvesting and Plant Fitness in the Field. Science 297, 91–93 (2002).

Liang J, Crowther TW, Picard N, Wiser S, Zhou M, Alberti G, Schulze E-D, McGuire AD, Bozzato F, Pretzsch H et al. Positive biodiversity-productivity relationship predominant in global forests. Science 354, aaf8957 (2016).

Lobo FA, de Barros MP, Dalmagro HJ, Dalmolin ÂC, Pereira WE, de Souza ÉC, Vourlitis GL, Rodríguez Ortíz CE. Fitting net photosynthetic light-response curves with Microsoft Excel — a critical look at the models. Photosynthetica 51, 445–456 (2013).

Long SP, Humphries S, Falkowski PG. Photoinhibition of Photosynthesis in Nature. Annual Review of Plant Physiology and Plant Molecular Biology 45, 633-62 (1994).

Loreau M, Hector A. Partitioning selection and complementarity in biodiversity experiments. Nature 412, 72–76 (2001).

Lovelock CE, Clough BF. Influence of solar radiation and leaf angle on leaf xanthophyll concentrations in mangroves. Oecologia 91, 518–525 (1992).

Maestre FT, Callaway RM, Valladares F, Lortie CJ. Refining the stress-gradient hypothesis for competition and facilitation in plant communities. Journal of Ecology 97, 199–205 (2009).

Mattila H, Valev D, Havurinne V, Khorobrykh S, Virtanen O, Antinluoma M, Mishra KB, Tyystjärvi E. Degradation of chlorophyll and synthesis of flavonols during autumn senescence—the story told by individual leaves. AoB Plants 10, (2018).

Monsi M, Saeki T. On the Factor Light in Plant Communities and its Importance for Matter Production. Ann Bot 95, 549–567 (2005).

Monteith JL, Moss CJ, Cooke GW, Pirie NW, Bell GDH. Climate and the efficiency of crop production in Britain. Philosophical Transactions of the Royal Society of London B: Biological Sciences 281, 277–294 (1977).

Montgomery RA, Goldstein G, Givnish TJ. Photoprotection of PSII in Hawaiian lobeliads from diverse light environments. Functional Plant Biol. 35, 595–605 (2008).

Murchie EH, Niyogi KK. Manipulation of Photoprotection to Improve Plant Photosynthesis. Plant Physiology 155, 86–92 (2011).

Niinemets Ü, Valladares F. Tolerance to Shade, Drought, and Waterlogging of Temperate Northern Hemisphere Trees and Shrubs. Ecological Monographs 76, 521–547 (2006).

Oehri J, Schmid B, Schaepman-Strub G, Niklaus PA. Biodiversity promotes primary productivity and growing season lengthening at the landscape scale. PNAS 114, 10160–10165 (2017).

Parent S, Messier C. A simple and efficient method to estimate microsite light availability under a forest canopy. Can. J. For. Res. 26, 151–154 (1996).

Pastenes C, Porter V, Baginsky C, Horton P, González J. Paraheliotropism can protect water-stressed bean (Phaseolus vulgaris L.) plants against photoinhibition. Journal of Plant Physiology 161, 1315–1323 (2004).

Pearcy RW, Muraoka H, Valladares F. Crown architecture in sun and shade environments: assessing function and trade-offs with a three-dimensional simulation model. New Phytologist 166, 791–800 (2005).

Pillai P, Gouhier TC. Not even wrong: the spurious measurement of biodiversity's effects on ecosystem functioning. Ecology 100, e02645 (2019).

Poorter H, Niinemets Ü, Ntagkas N, Siebenkäs A, Mäenpää M, Matsubara S, Pons TL. A meta-analysis of plant responses to light intensity for 70 traits ranging from molecules to whole plant performance. New Phytologist 223, 1073–1105 (2019).

Potvin C, Gotelli NJ. Biodiversity enhances individual performance but does not affect survivorship in tropical trees. Ecology Letters 11, 217–223 (2008).

Ramírez-Valiente JA, Koehler K, Cavender-Bares J. Climatic origins predict variation in photoprotective leaf pigments in response to drought and low temperatures in live oaks (Quercus series Virentes). Tree Physiology 35, 521–534 (2015).

Renner SS, Zohner CM. The occurrence of red and yellow autumn leaves explained by regional differences in insolation and temperature. New Phytologist 224, 1464–1471 (2019).

Ryser P, Eek L. Consequences of phenotypic plasticity vs. interspecific differences in leaf and root traits for acquisition of aboveground and belowground resources. American Journal of Botany 87, 402–411 (2000).

Savage, J., J. Cavender-Bares, and A. Verhoeven. Habitat generalists and wetland specialists in the genus Salix vary in their photoprotective responses to drought. Functional Plant Biology 36, 300–309 (2009).

Schall P, Lödige C, Beck M, Ammer C. Biomass allocation to roots and shoots is more sensitive to shade and drought in European beech than in Norway spruce seedlings. Forest Ecology and Management 266, 246–253 (2012).

Schymanski SJ, Or D, Zwieniecki M. Stomatal Control and Leaf Thermal and Hydraulic Capacitances under Rapid Environmental Fluctuations. PLOS ONE 8, e54231 (2013).

Semchenko M, Lepik M, Götzenberger L, Zobel K. Positive effect of shade on plant growth: amelioration of stress or active regulation of growth rate? Journal of Ecology 100, 459–466 (2012).

Tilman D. Secondary Succession and the Pattern of Plant Dominance Along Experimental Nitrogen Gradients. Ecological Monographs 57, 189–214 (1987).

Tilman D, Isbell F, Cowles JM. Biodiversity and Ecosystem Functioning. Annual Review of Ecology, Evolution, and Systematics 45, 471–493 (2014).

Tobner CM, Paquette A, Gravel D, Reich PB, Williams LJ, Messier C. Functional identity is the main driver of diversity effects in young tree communities. Ecol Lett 19, 638–647 (2016).

Valiente-Banuet A, Verdú M, Valladares F, García-Fayos P. Functional and evolutionary correlations of steep leaf angles in the mexical shrubland. Oecologia 163, 25–33 (2010).

Valladares F, Pugnaire FI. Tradeoffs Between Irradiance Capture and Avoidance in Semi-arid Environments Assessed with a Crown Architecture Model. Annals of Botany 83, 459–469 (1999).

Watling JR, Robinson SA, Woodrow IE, Osmond CB. Responses of Rainforest Understorey Plants to Excess Light during Sunflecks. Australian Journal of Plant Physiology 24, 17–25 (1997).

Werner C, Correia O, Beyschlag W. Two different strategies of Mediterranean macchia plants to avoid photoinhibitory damage by excessive radiation levels during summer drought. Acta Oecologica 20, 15–23 (1999).

Williams LJ, Paquette A, Cavender-Bares J, Messier C, Reich PB. Spatial complementarity in tree crowns explains overyielding in species mixtures. Nature Ecology & Evolution 1, 0063 (2017).

Wong CYS, Gamon JA. Three causes of variation in the photochemical reflectance index (PRI) in evergreen conifers. New Phytol 206, 187–195 (2015).

Wright AJ, Wardle DA, Callaway R, Gaxiola A. The Overlooked Role of Facilitation in Biodiversity Experiments. Trends in Ecology & Evolution 32, 383–390 (2017).

Wujeska A, Bossinger G, Tausz M. Responses of foliar antioxidative and photoprotective defence systems of trees to drought: a meta-analysis. Tree Physiology 33, 1018–1029 (2013).

Zemp DC, Gérard A, Hölscher D, Ammer C, Irawan B, Sundawati L, Teuscher M, Kreft H. Tree performance in a biodiversity enrichment experiment in an oil palm landscape. Journal of Applied Ecology 56, 2340–2352 (2019).

Zhu X-G, Ort DR, Whitmarsh J, Long SP. The slow reversibility of photosystem II thermal energy dissipation on transfer from high to low light may cause large losses in carbon gain by crop canopies: a theoretical analysis. J Exp Bot 55, 1167–1175 (2004).

Tables

Table 1: Characteristics of species in FAB. Except for *B. papyrifera*, broadleaf species tended to grow slower than needleleaf conifers. Shade tolerance is drawn from Niinemets and Valladares (2006), who evaluated it along a 1-5 scale where higher values indicate an ability to grow under lower light.

Scientific name	Species code	Common name	Family	Leaf form	Mean RGR in monoculture, 2013-6 (/year)	Shade tolerance	Partner in shaded biculture
Acer negundo	ACNE	Box elder	Sapindaceae	Broadleaf	0.039	3.47	None
Acer rubrum	ACRU	Red maple	Sapindaceae	Broadleaf	0.379	3.44	*Pinus banksiana*
Betula papyrifera	BEPA	Paper birch	Betulaceae	Broadleaf	1.272	1.54	*Pinus banksiana*
Juniperus virginiana	JUVI	Eastern redcedar	Cupressaceae	Needleleaf	0.975	1.28	NA
Pinus banksiana	PIBA	Jack pine	Pinaceae	Needleleaf	2.288	1.36	NA
Pinus resinosa	PIRE	Red pine	Pinaceae	Needleleaf	1.619	1.89	NA
Pinus strobus	PIST	White pine	Pinaceae	Needleleaf	1.722	3.21	NA
Quercus alba	QUAL	White oak	Fagaceae	Broadleaf	0.735	2.85	*Pinus strobus*
Quercus ellipsoidalis	QUEL	Northern pin oak	Fagaceae	Broadleaf	0.722	NA	*Pinus strobus*
Quercus macrocarpa	QUMA	Bur oak	Fagaceae	Broadleaf	0.547	2.71	*Betula papyrifera*
Quercus rubra	QURU	Northern red oak	Fagaceae	Broadleaf	0.505	2.75	*Pinus strobus*
Tilia americana	TIAM	American basswood	Tiliaceae	Broadleaf	0.724	3.98	*Pinus strobus*

Figure captions

Fig. 1: (A) Consider two hypothetical photosynthetic light-response curves of unstressed (blue) and photoinhibited (red) plants, where the unstressed plant's neighbors reduce the amount of light it absorbs. Given a light-response curve, an instantaneous reduction in light tends to reduce photosynthetic rates (represented by the small black arrow along the red curve). However, if a long-term reduction in light spares the plant from chronic photoinhibition, it can alter the parameters of the curve such that carbon assimilation at any given instantaneous light level is greater (represented by the small black vertical arrow). The balance (represented by the large dashed arrow) may either increase or reduce net carbon assimilation.

(B) To allow us to compare photosynthetic rates visually, we can put the two light-response curves on a common *x*-axis that represents light arriving at the top of the canopy. To do this, we need to scale the blue light response curve horizontally to account for the fact that when the stressed plant receives the amount of light corresponding to the red dashed line in (A), the unstressed plant receives a proportionally lower amount, here represented by the blue dashed line. By stretching the blue curve proportionally such that these two lines coincide, we can compare the true estimated photosynthetic rates at a given light availability.

Fig. 2: Relative growth rate (RGR) of woody stem volume in individuals of each species between fall 2016 and 2018 as a function of the total stem volume of all neighbors. Gray dots represent individuals, and the regression line is fit through the individual-level data. Large colored dots are aggregated to the plot scale, as described in the main text, and color-coded by treatment. A shaded biculture is a plot in which the focal broadleaf species grows with either a conifer or *B. papyrifera* (unless *B. papyrifera* is the focal broadleaf species). An open biculture is a plot in which the focal broadleaf grows with another broadleaf species (other than *B. papyrifera*).

Fig. 3: Mass-based photosynthetic light-response curves for four broadleaf species. The left panels display photosynthetic rates as a function of chamber light intensity; the right panels represent an estimate of realized photosynthetic rates as a function of light intensity at the top of the canopy, after accounting for light interception by neighbors (as in Fig. 1B). Species are arranged from the least shade-tolerant (*B. papyrifera*) to the most (*T. americana*). Error bars in left panels are ± 1 SE.

Fig. 4: Dark-acclimated F_v/F_m, qN, ϕ_{NO}, and PRI as a function of relative light availability across species and treatments.

Fig. 5: Compared to shade-intolerant species, shade-tolerant species show greater declines in dark-acclimated F_v/F_m and smaller increases in qN as light availability increases. A_{sat} derived from light-response curves correlates positively and strongly with dark-acclimated F_v/F_m; slopes are statistically indistinguishable among species.

Fig. 6: Timing of fall leaf abscission in monoculture and shaded biculture treatments of *T. americana*.

Fig. 7: Top leaf angles of *A. rubrum* (left), *Q. ellipsoidalis* (middle), and *T. americana* (right) across treatments.

Fig. S1: Example images of *Tilia americana* in shaded biculture (top) and monoculture (bottom). Red scale bars represent about 1 m in the foreground.

Fig. S2: Growth of woody stem volume in individuals of each species between fall 2017 and 2018 as a function of the total stem volume of all neighbors. Gray dots represent individuals, while colored dots are aggregated to the plot scale and color-coded by treatment. Two regression lines are fit: One (blue) to all data, and one (red) excluding trees that died between 2017 and 2018.

Fig. S3: Responses of ETR and stomatal conductance to light availability for the four focal broadleaf species. Error bars are ± 1 SE.

Fig. S4: An estimate of total carbon assimilation across species and treatments throughout the month of July, calculated by applying a time series of solar radiation from a nearby weather station as inputs to our ambient light-response curves.

Fig. S5: A ternary plot depicting variation among species and treatments in ϕ_{PSII}, ϕ_{NPQ}, and ϕ_{NO}, as calculated using the lake model derivations of Kramer et al. (2004). These three quantities describe light energy dissipation through photochemistry, through non-photochemical quenching, and through non-regulated dissipation, respectively. A thick dashed line represents 0.83 the theoretical maximum efficiency of PSII posited in Tietz et al. (2017). Deviations from this line represent increasingly high ϕ_{NO}, which can result in photodamage.

Fig. S6: Water potential before dawn (top) and at midday (bottom) among species and treatments.

Figures

Fig. 1

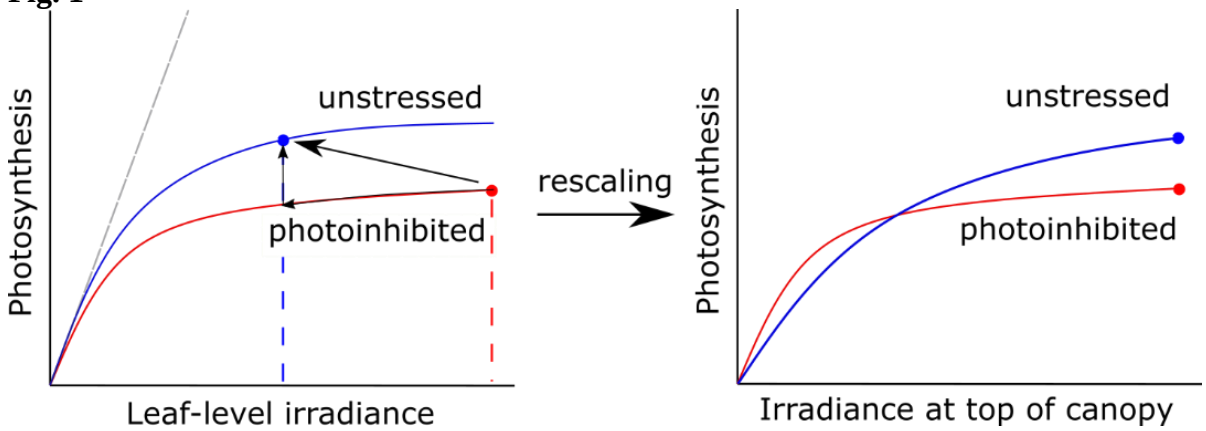

Fig. 2

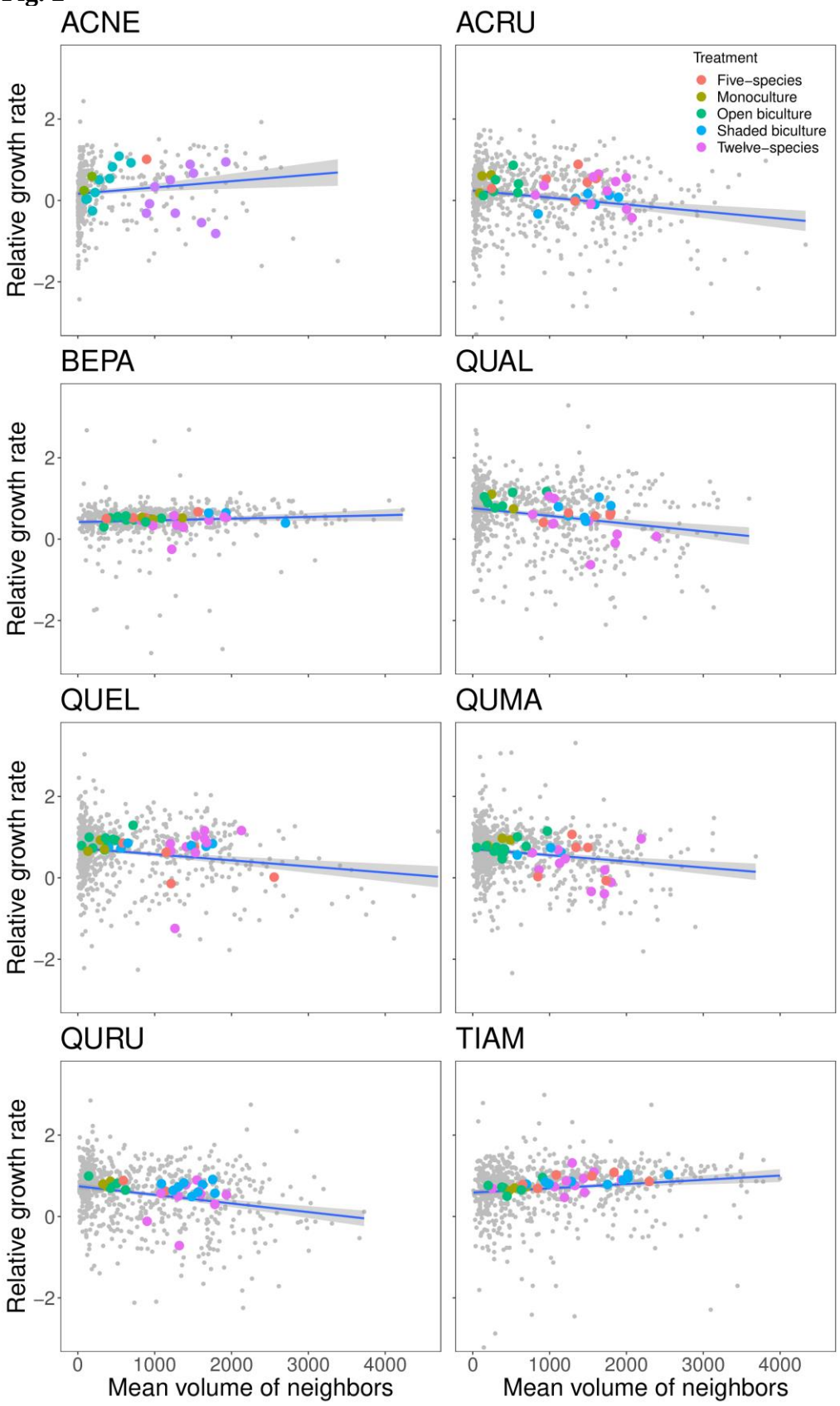
ACNE
ACRU
BEPA
QUAL
QUEL
QUMA
QURU
TIAM
Treatment
Five−species
Monoculture
Open biculture
Shaded biculture
Twelve−species
Relative growth rate
2
0
−2
0
1000
2000
3000
4000
Mean volume of neighbors

Fig. 3

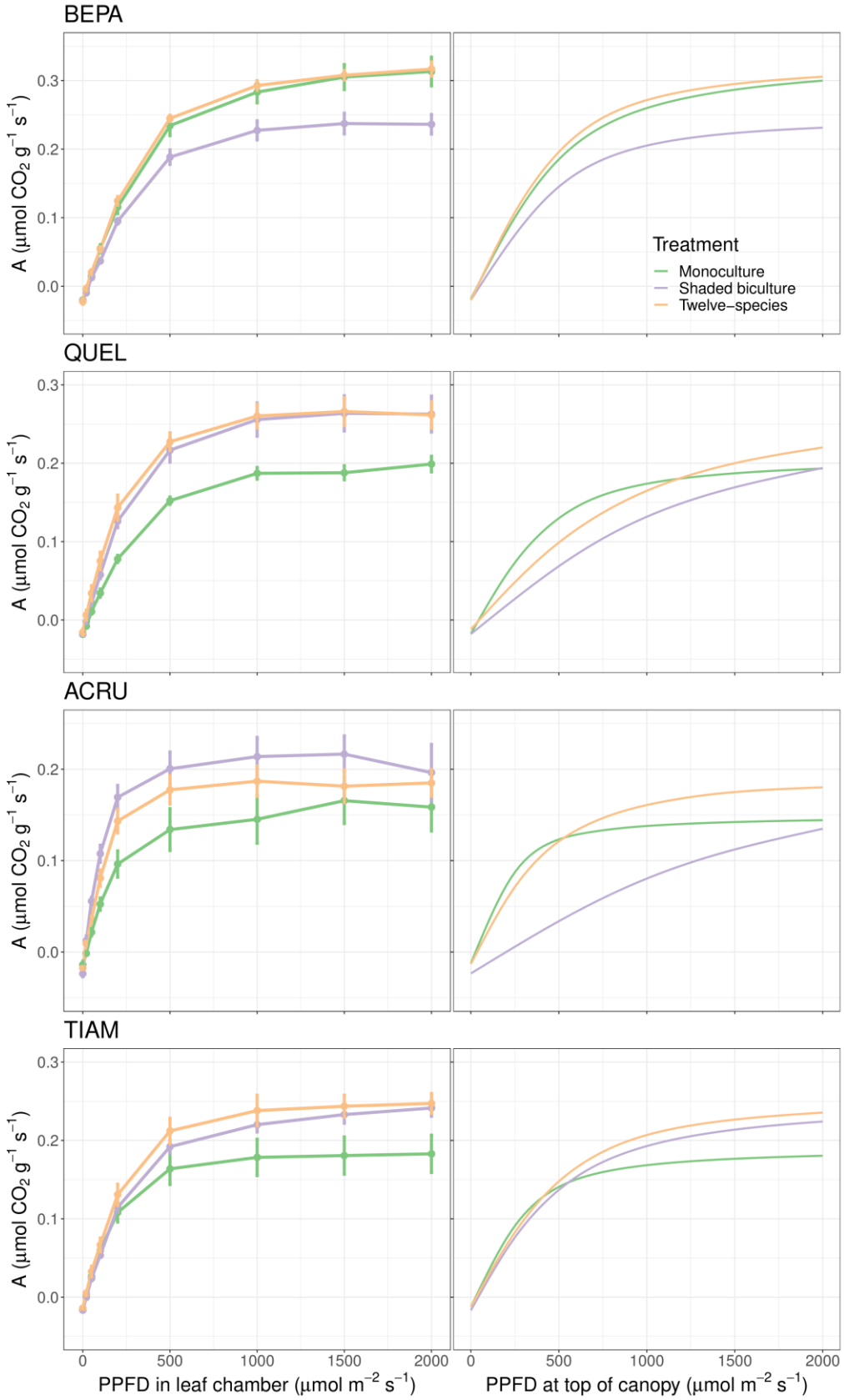
BEPA
QUEL
ACRU
TIAM
A (µmol CO2 g−1 s−1)
0.0
0.1
0.2
0.3
0
500
1000
1500
2000
PPFD in leaf chamber (µmol m−2 s−1)
PPFD at top of canopy (µmol m−2 s−1)
Treatment
Monoculture
Shaded biculture
Twelve−species

1089 **Fig. 4**

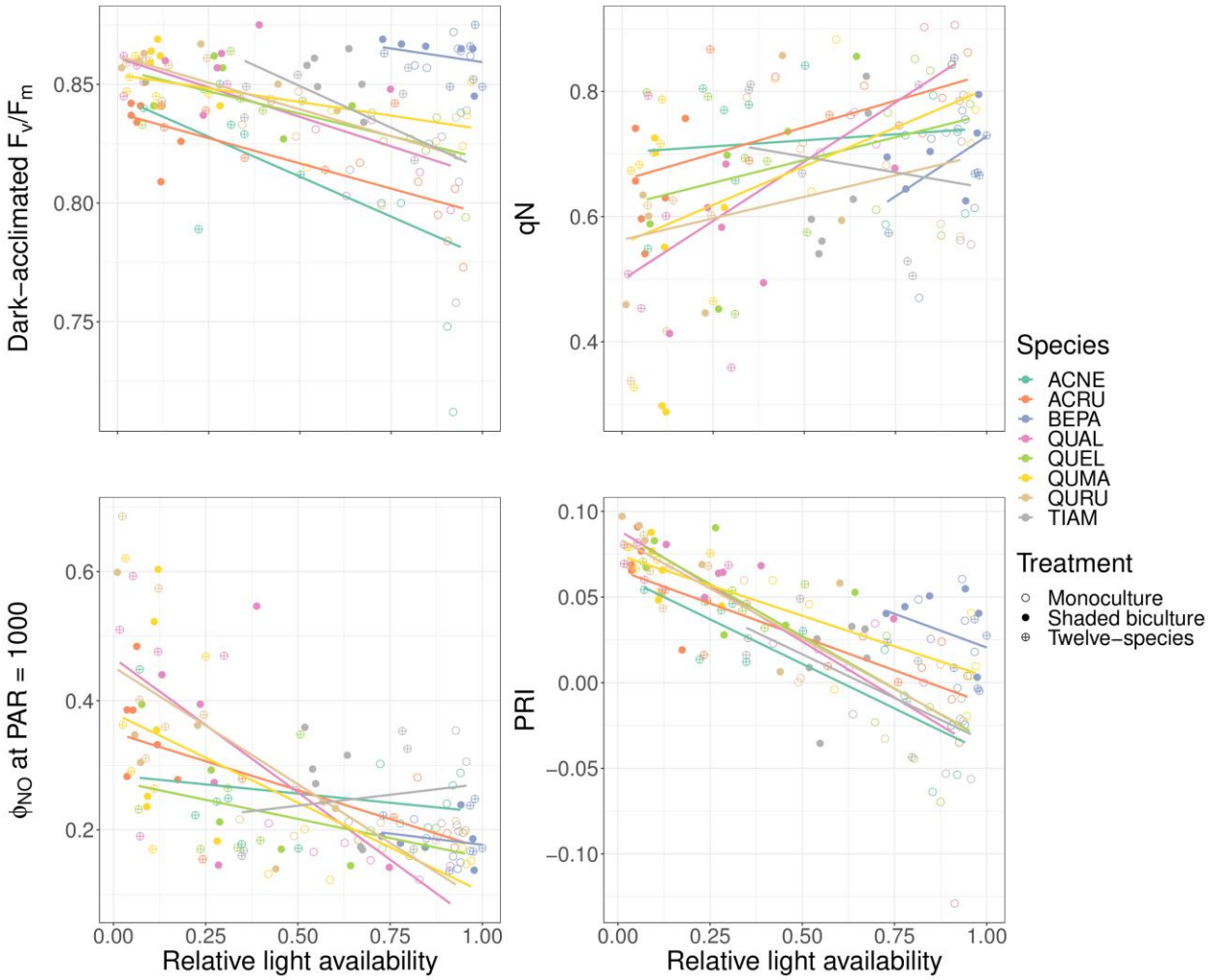

1090
1091
1092
1093
1094
1095
1096
1097
1098
1099
1100
1101
1102
1103
1104
1105
1106
1107
1108

Fig. 5

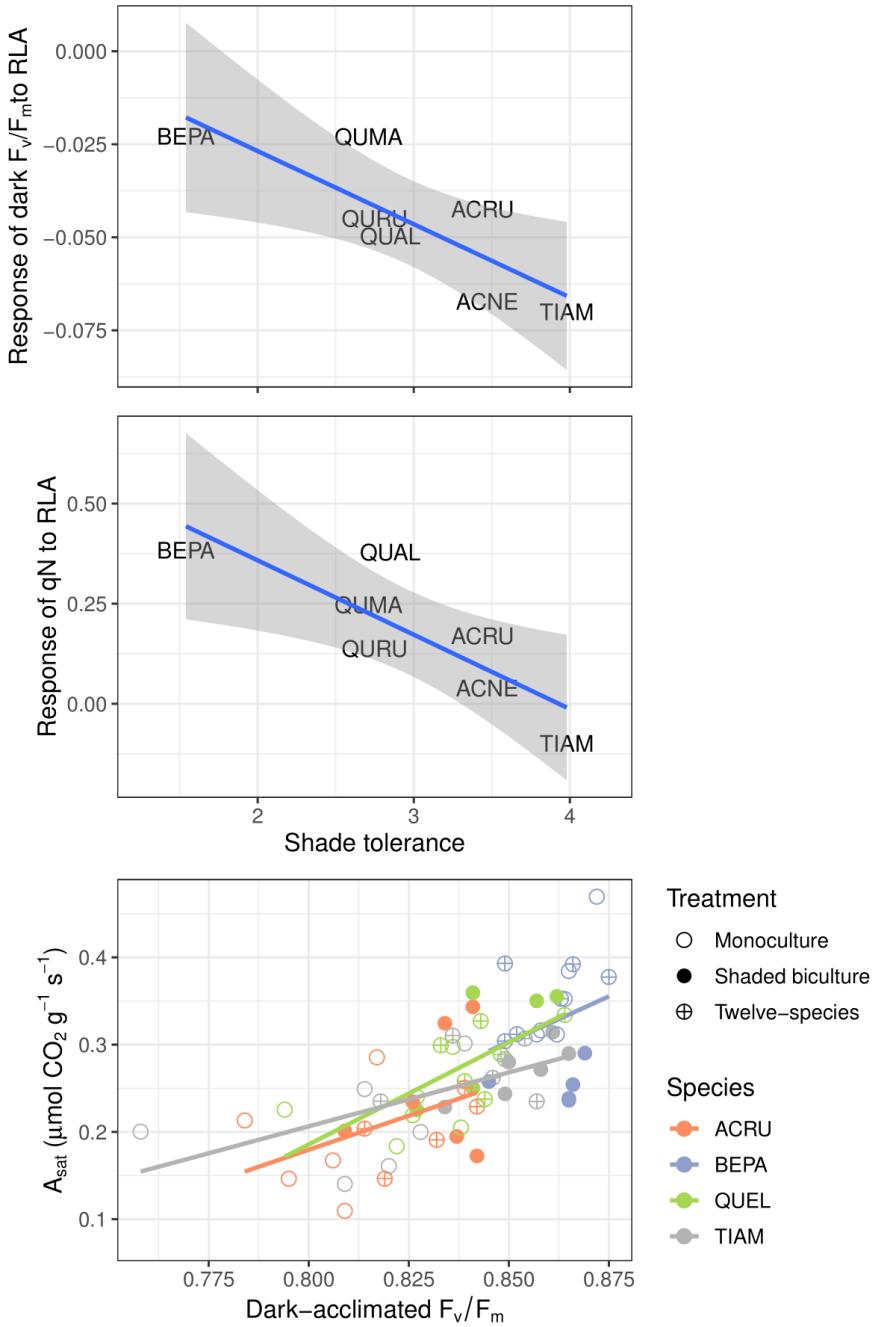
Response of dark F_v/F_m to RLA
0.000
−0.025
−0.050
−0.075
BEPA
QUMA
QURU
QUAL
ACRU
ACNE
TIAM
Response of qN to RLA
0.50
0.25
0.00
BEPA
QUAL
QUMA
QURU
ACRU
ACNE
TIAM
2
3
4
Shade tolerance
A_{sat} (µmol CO_2 g^{-1} s^{-1})
0.4
0.3
0.2
0.1
0.775
0.800
0.825
0.850
0.875
Dark−acclimated F_v/F_m
Treatment
Monoculture
Shaded biculture
Twelve−species
Species
ACRU
BEPA
QUEL
TIAM

Fig. 6

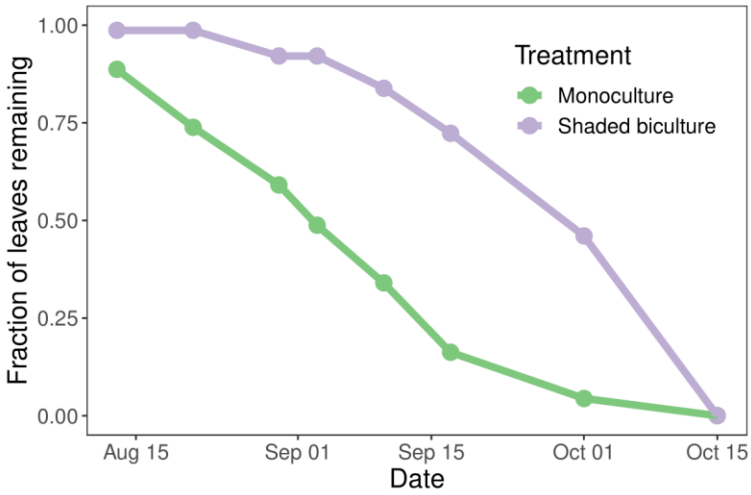
Treatment
Monoculture
Shaded biculture
Fraction of leaves remaining
1.00
0.75
0.50
0.25
0.00
Aug 15
Sep 01
Sep 15
Oct 01
Oct 15
Date

Fig. 7

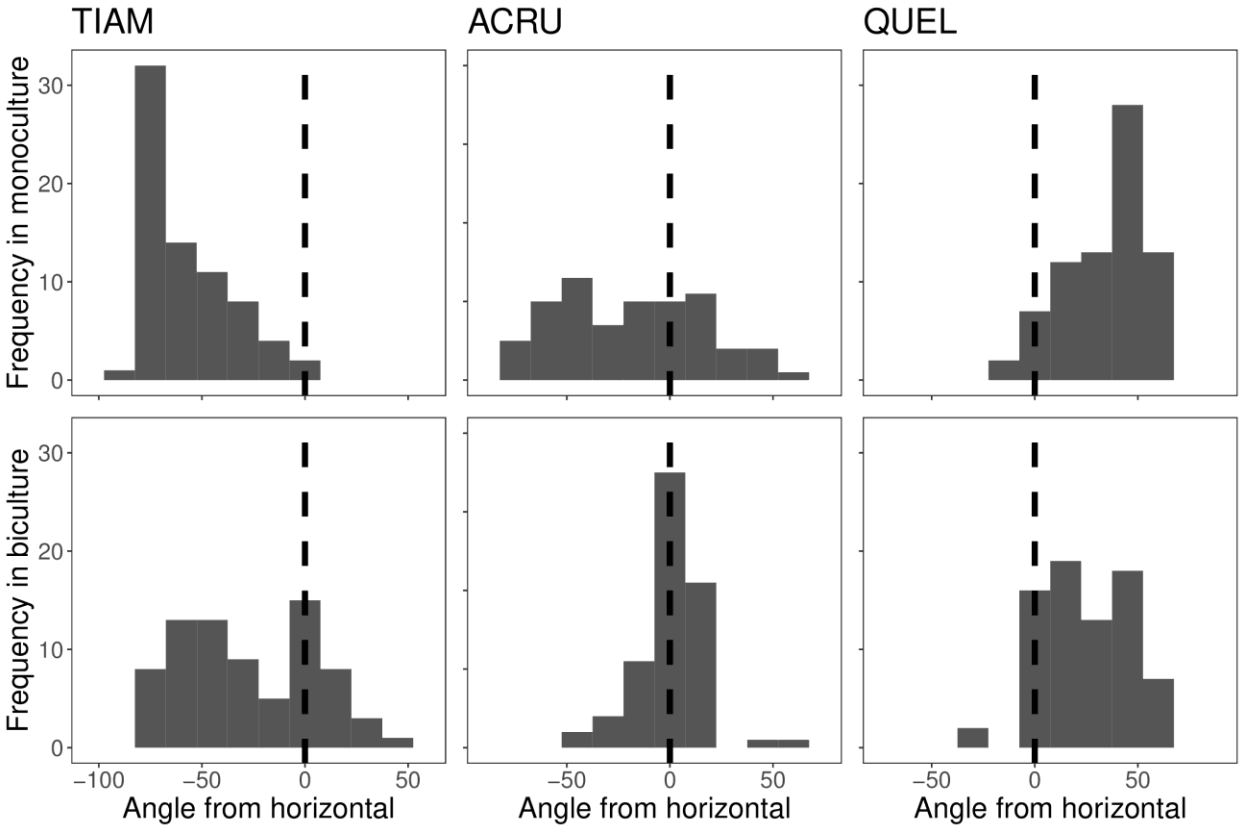
TIAM
ACRU
QUEL
Frequency in monoculture
Frequency in biculture
30
20
10
0
−100
−50
0
50
Angle from horizontal

Supplement to: "Throwing shade: Physiological responses to light mediate competition and facilitation in a tree diversity experiment"

Materials and Methods

Photosynthetic light-response curve methods

We measured photosynthetic-light response curves from the four focal species (*Acer negundo*, *Betula papyrifera*, *Quercus ellipsoidalis*, and *Tilia americana*) during July 2018 using an LI-6400 gas exchange system (LI-COR BioSciences, Lincoln, NE) with a 6400-40 Leaf Chamber Fluorometer head. From each tree (n = 72 total), we selected a fully expanded, sun-exposed leaf with no visible sign of disease or herbivory. We noted the angle of each leaf relative to horizontal to the nearest 15˚ before beginning measurements. Each curve had nine steps in descending order of brightness: 2000, 1500, 1000, 500, 200, 100, 50, 20, and 0 µmol m^{-2} s^{-1}.

During each curve, we controlled environmental conditions to reduce the immediate effects of environmental conditions, other than light, on stomatal conductance. We maintained relative humidity at a favorable level, typically between 65 and 75%, and kept block temperature as close as possible to 25 ˚C. The reference CO_2 concentration remained at 400±10 ppm. We kept each leaf in the chamber for at least five minutes before beginning each curve. We checked that outputs were stable and matched IRGAs before each measurement.

While we sought to control environmental conditions in the chamber, any remaining differences among treatments could, in theory, contribute to the differences we observe in photosynthetic function. During light-response curves, we found no difference among treatments in leaf-to-air VPD within the chamber. There were significant but slight differences in leaf temperature inside the chamber; leaves in monoculture, shaded biculture, and twelve-species plots had average temperatures of 27.7 ˚C, 26.5 ˚C, and 27.0 ˚C, respectively. Previous studies on some of the same species in Minnesota have typically found thermal optima below 26 ˚C (Sendall et al. 2015). However, while cooler leaves may be closer to

thermal optima, the small differences in temperature we observed seem unlikely to explain much of the observed variation in photosynthetic rates within the leaf chamber.

In all but five light-response curves, we also used a saturating pulse to measure light-acclimated chlorophyll fluorescence at each light level. These data allowed us to calculate ϕ_{PSII}, a measure of the efficiency of Photosystem II (PSII) at each actinic light level, as:

$$\phi_{PSII} = \frac{F_m' - F_s}{F_m'}$$

where F_s is the steady-state fluorescence yield under actinic light, and F_m' is the maximum fluorescence yield of the actinic light-acclimated sample following a saturating light pulse, which temporarily closes all PSII reaction centers. From this parameter, we could calculate electron transport rate as:

$$ETR = \phi_{PSII} \times PPFD \times 0.42 \times 0.5$$

where PPFD is photosynthetic photon flux density (the light level inside the chamber, in μmol m^{-2} s^{-1}), 0.42 is an estimate of leaf absorptance, and 0.5 is an estimate of the fraction of photons that are captured by PSII rather than PSI. Electron transport rate is a key parameter because electron transport is one of the main steps that is capable of limiting photosynthesis (Farquhar et al. 1980), especially when light availability or PSII efficiency are low.

Chlorophyll fluorescence procedure

As described in the main text, we used dark- and light-acclimated measurements of chlorophyll fluorescence to calculate several derived parameters, from which we make inferences about photosynthetic and photoprotective function. Most importantly, we wanted to assess: (1) capacity for non-photochemical quenching, as measured through the parameters qN or NPQ; and (2) the partitioning of light energy among different processes, as assessed using the quantum yields ϕ_{PSII}, ϕ_{NPQ}, and ϕ_{NO}.

These derived chlorophyll fluorescence parameters are calculated from a few basic measurements taken during the dark- and light-acclimated measurements, including: F_o, the minimum fluorescence yield of a dark-acclimated sample with all PSII reaction centers open; F_o', the minimum fluorescence yield of a

light-acclimated sample with all PSII reaction centers open (following far-red light exposure); and F_m, the maximum fluorescence yield of a dark-acclimated sample following a saturating pulse. F_v, the variable fluorescence yield of a dark-acclimated sample, is calculated as $F_m - F_o$.

The parameters qN and NPQ are meant to indicate the rate constant of the thermal dissipation of energy from PSII (Bilger and Schreiber 1986; Bilger and Björkman 1990). These parameters increase with the use of NPQ to dissipate light—in this case, under exposure to 1000 µmol m^{-2} s^{-1}. They are calculated, respectively, as:

$$qN = 1 - \frac{F_m' - F_o'}{F_m - F_o}; NPQ = \frac{F_m - F_m'}{F_m'}$$

In our dataset, qN is highly correlated (R^2 = 0.96) with the natural logarithm of NPQ; we chose to report qN to easily visualize variation among leaves with low NPQ and to help satisfy the error term normality assumption of OLS regression.

The quantum yields ϕ_{PSII}, ϕ_{NPQ}, and ϕ_{NO} represent the proportions of absorbed light energy that are dissipated through photochemical processes, non-photochemical quenching, and non-regulated dissipation, respectively. As proportions, these quantum yields sum to 1. We calculated these parameters following the "lake model" derivation of Kramer et al. (2004), which treats photosynthetic reaction centers as connected by shared antennae. We achieve qualitatively similar results using the simpler analogues found in Hendricksen et al. (2005).

The parameter ϕ_{PSII} is as calculated above (Supplemental Methods, *Photosynthetic light-response curve procedure*). In the derivation from Kramer et al. (2004), ϕ_{NPQ} and ϕ_{NO} are calculated using the parameter qL, an estimate of the fraction of open PSII reaction centers. qL is calculated as:

$$qL = \frac{F_m' - F_s}{F_m' - F_o'} \frac{F_o'}{F_s}$$

Given this parameter, we can calculate ϕ_{NO} as:

$$\phi_{NO} = \frac{1}{NPQ + 1 + qL\left(\frac{F_m}{F_o} - 1\right)}$$

and given the other two quantum yields, we can calculate ϕ_{NPQ} as:

$$\phi_{NPQ} = 1 - \phi_{PSII} - \phi_{NO}$$

Many researchers, including Murchie and Lawson (2013) and Tietz et al. (2017) treat ~0.83 as a theoretical maximum of ϕ_{PSII} or dark-acclimated F_v/F_m after a period of dark-acclimation long enough to reduce non-photochemical quenching to zero. Similarly, one may treat ~0.83 as a theoretical maximum of $\phi_{PSII} + \phi_{NPQ}$, deviations from which indicate high ϕ_{NO}, and thus, a declining ability to dissipate light energy in a regulated way. We indicate this putative maximum in our ternary plot of the quantum yields (Fig. S5).

References

Bilger W, Björkman O. Role of the xanthophyll cycle in photoprotection elucidated by measurements of light-induced absorbance changes, fluorescence and photosynthesis in leaves of *Hedera canariensis*. Photosynthesis Research 25, 173–185 (1990).

Bilger W, Schreiber U. Energy-dependent quenching of dark-level chlorophyll fluorescence in intact leaves. Photosynthesis Research 10, 303–308 (1986).

Farquhar GD, von Caemmerer S, Berry JA. A biochemical model of photosynthetic CO2 assimilation in leaves of C 3 species. Planta 149, 78–90 (1980).

Hendrickson L, Förster B, Pogson BJ, Chow WS. A simple chlorophyll fluorescence parameter that correlates with the rate coefficient of photoinactivation of Photosystem II. Photosynthesis Research 84, 43–49 (2005).

Kramer DM, Johnson G, Kiirats O, Edwards GE. New Fluorescence Parameters for the Determination of QA Redox State and Excitation Energy Fluxes. Photosynthesis Research 79, 209–218 (2004).

Murchie EH, Lawson T. Chlorophyll fluorescence analysis: a guide to good practice and understanding some new applications. Journal of Experimental Botany 64, 3983–3998 (2013).

Sendall, KM, Reich PB, Zhao C, Jihua H, Wei X, Stefanski A, Rice K, Rich RL, Montgomery RA. Acclimation of photosynthetic temperature optima of temperate and boreal tree species in response to experimental forest warming. Global Change Biology 21, 1342–1357 (2015).

Tietz S, Hall CC, Cruz, JA, Kramer DM. NPQ(T): a chlorophyll fluorescence parameter for rapid estimation and imaging of non-photochemical quenching of excitons in photosystem-II-associated antenna complexes. Plant, Cell & Environment 40, 1243–1255 (2017).

Fig. S1

Fig. S2

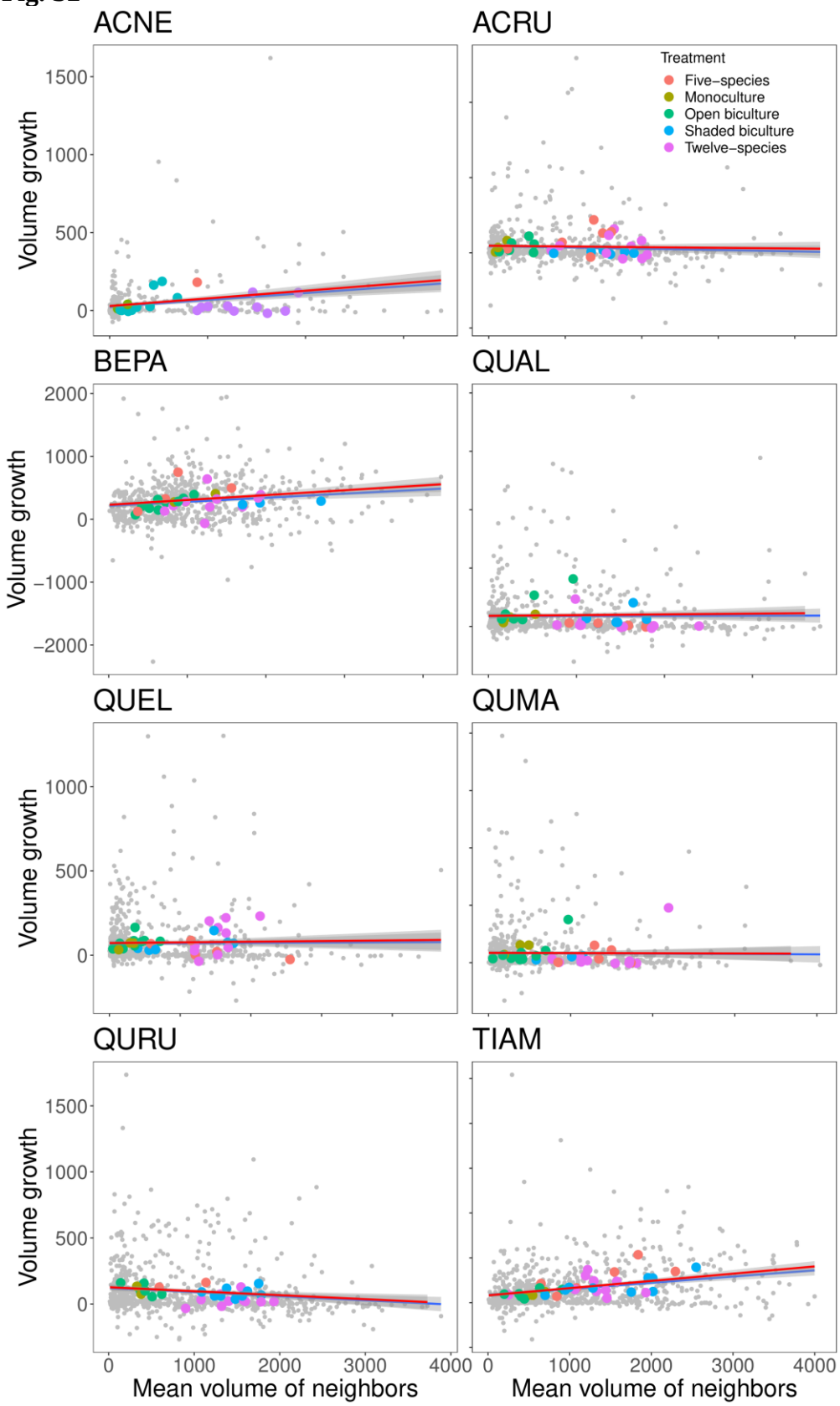
ACNE
ACRU
BEPA
QUAL
QUEL
QUMA
QURU
TIAM
Treatment
Five−species
Monoculture
Open biculture
Shaded biculture
Twelve−species
Volume growth
Mean volume of neighbors

Fig. S3

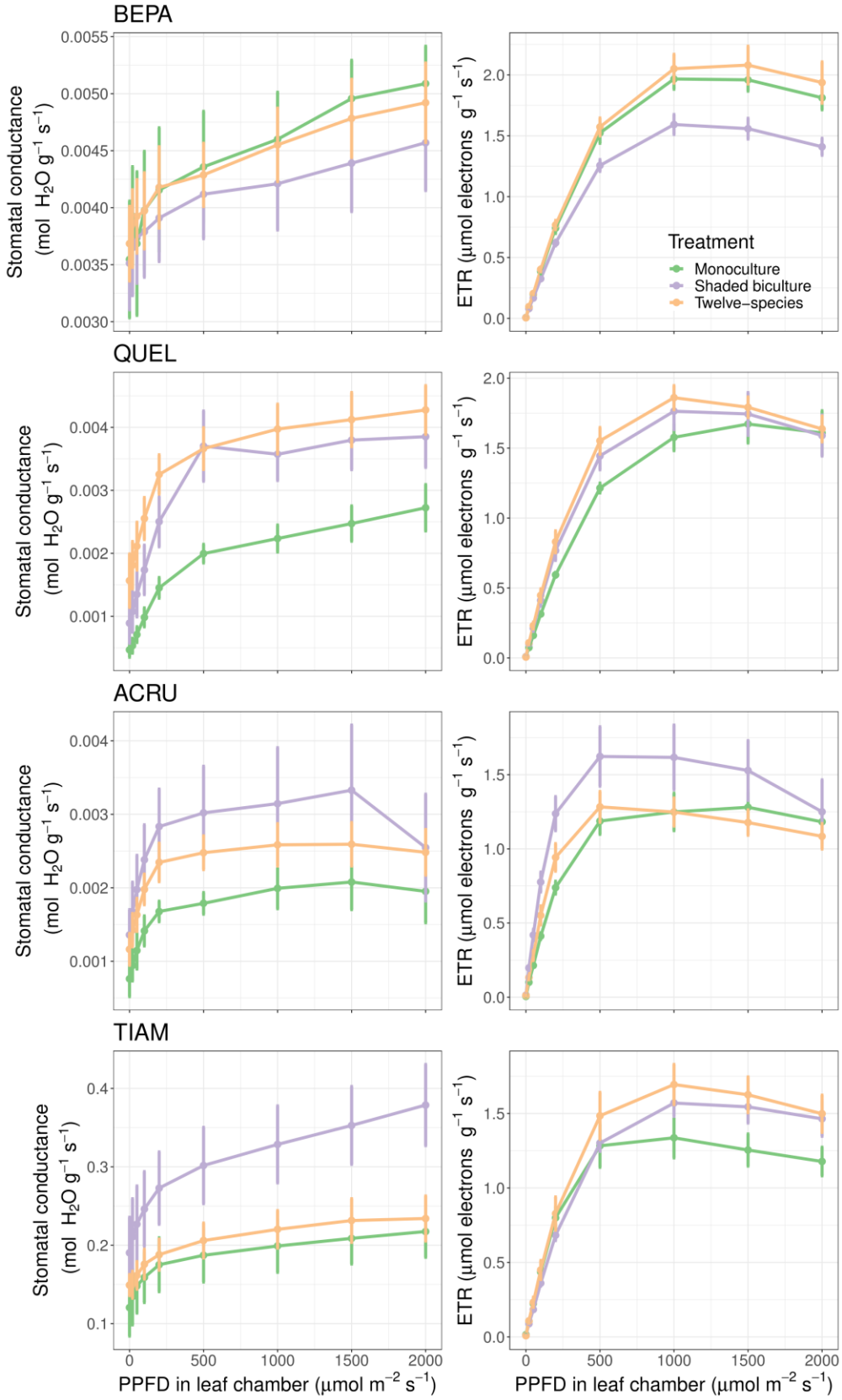
BEPA
QUEL
ACRU
TIAM
Stomatal conductance (mol H2O g−1 s−1)
ETR (µmol electrons g−1 s−1)
Treatment
Monoculture
Shaded biculture
Twelve−species
PPFD in leaf chamber (µmol m−2 s−1)

Fig. S4

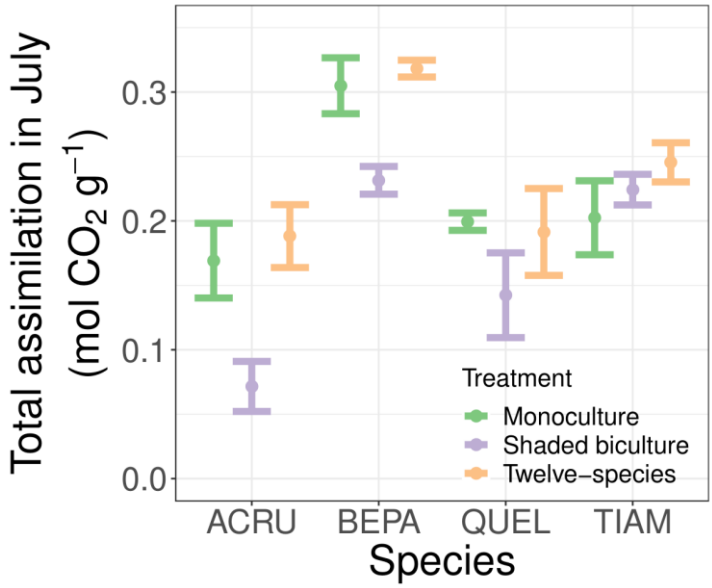
Total assimilation in July
(mol CO2 g−1)
0.0
0.1
0.2
0.3
ACRU
BEPA
QUEL
TIAM
Species
Treatment
Monoculture
Shaded biculture
Twelve−species

Fig. S5

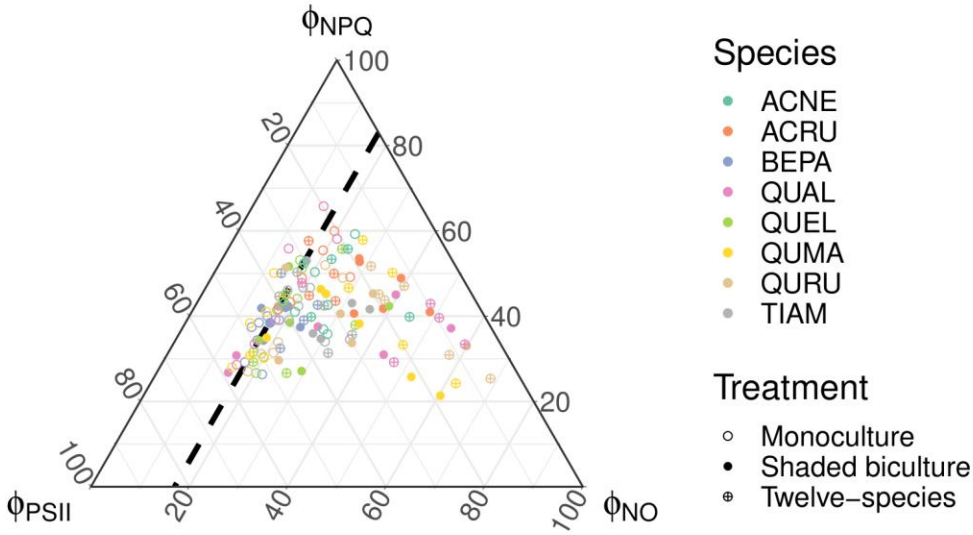
ϕNPQ
ϕPSII
ϕNO
20
40
60
80
100
Species
ACNE
ACRU
BEPA
QUAL
QUEL
QUMA
QURU
TIAM
Treatment
Monoculture
Shaded biculture
Twelve−species

Fig. S6

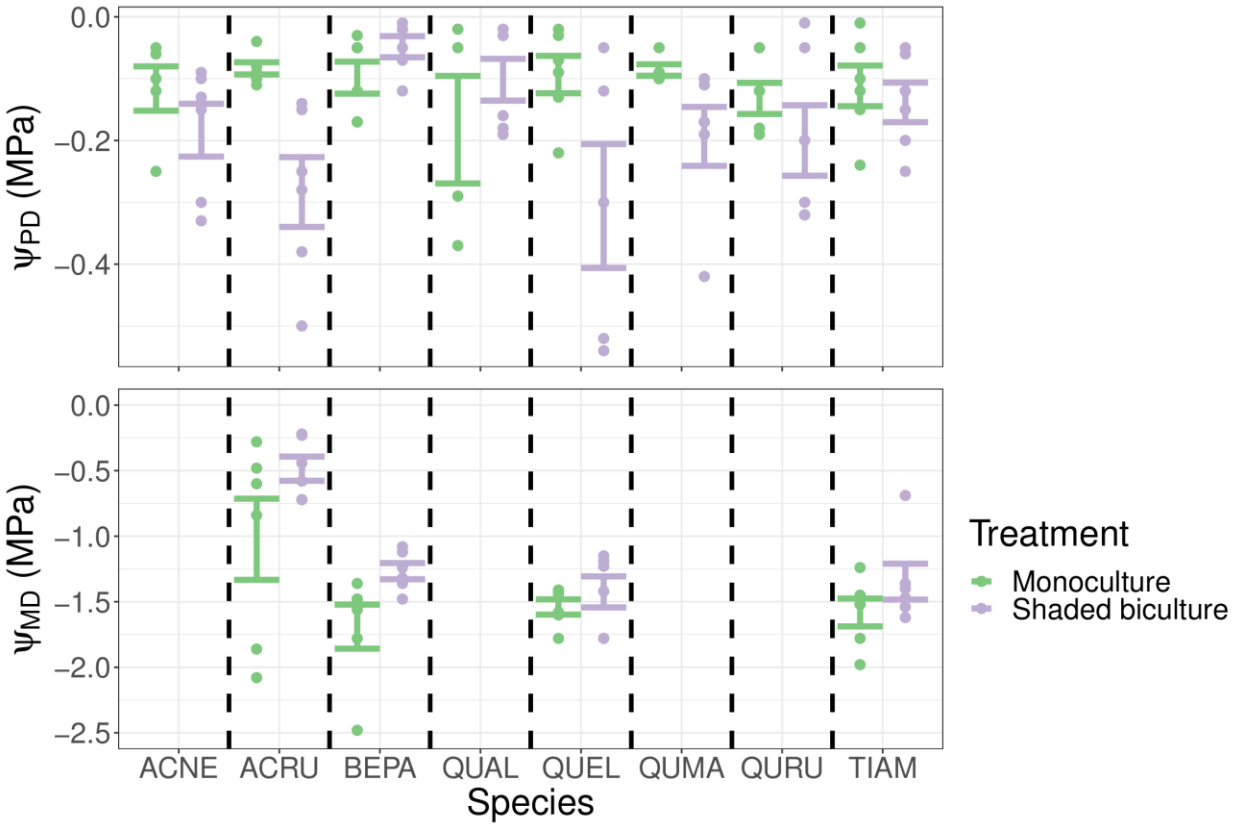
0.0
−0.2
−0.4
ψPD (MPa)
0.0
−0.5
−1.0
−1.5
−2.0
−2.5
ψMD (MPa)
ACNE
ACRU
BEPA
QUAL
QUEL
QUMA
QURU
TIAM
Species
Treatment
Monoculture
Shaded biculture